

International Journal of Modern Physics A
© World Scientific Publishing Company

Lattice QCD at the End of 2003

Thomas DeGrand

Department of Physics, University of Colorado, Boulder, CO 80309 USA

I review recent developments in lattice QCD. I first give an overview of its formalism, and then discuss lattice discretizations of fermions. We then turn to a description of the quenched approximation and why it is disappearing as a vehicle for QCD phenomenology. I describe recent claims for progress in simulations which include dynamical fermions and the interesting theoretical problems they raise. I conclude with brief descriptions of the calculations of matrix elements in heavy flavor systems and for kaons.

Keywords: QCD; lattice; weak matrix elements

1. Introduction

Lattice regulated quantum field theory supplemented by numerical simulations is a major source of information about Quantum Chromodynamics (QCD), the theory of the strong interactions. This article is an overview of lattice QCD, with a target audience of particle physicists who do not do lattice calculations themselves, but might be “users” of them. Since lattice QCD is a mature field¹, most work in lattice QCD represents evolutionary progress, not revolutionary breakthroughs. But lattice QCD is presently going through a transition phase, as a long-used approximation to QCD (the quenched approximation) becomes increasingly problematic, and numerical studies of QCD which include the effects of dynamical quarks are beginning to produce interesting numbers – and their own interesting questions of principle.

Most lattice reviews –like most lattice calculations – are fixated on numbers, the values of reduced matrix elements computed at physical values of quark masses. Numbers are important, and the lattice can be the best source of some specific (model-independent) predictions of QCD. However, numbers evolve and become obsolete. I think it will be more interesting to take a more impressionistic view of lattice QCD, and concentrate on how the calculations are done. There are a lot of ways that they can fail, and phenomenologists who are going to use lattice determinations of reduced matrix elements in their own work ought to be aware of the potential weaknesses in them.

I will begin with a quick overview of lattice methodology: how to go from a continuum action to a lattice calculation, and then get back to the continuum. Next, I will describe methods for putting fermions on the lattice. A lot has happened here

2 *DeGrand*

since the last textbooks were written. I will then describe the quenched approximation (which is about to disappear as a source of quantitative lattice predictions) and tell you about recent work with dynamical fermions, which is certainly in a very peculiar state. I will then give an overview of two kinds of standard model tests, first heavy flavor physics, and then weak matrix elements of kaons. I will not discuss QCD thermodynamics, lattice-motivated scenarios of confinement or chiral symmetry breaking, or $N_c \neq 3$.

2. A superficial overview of lattice methodology

2.1. *Lattice Variables and Actions*

In order to perform calculations in quantum field theory it is necessary to control their ultraviolet divergences. The lattice is a space-time cutoff which eliminates all degrees of freedom from distances shorter than the lattice spacing a . As with any regulator, it must be removed after renormalization. Contact with experiment only exists in the continuum limit, when the lattice spacing is taken to zero. Other regularization schemes are tied closely to perturbative expansions: one calculates a process to some order in a coupling constant; divergences are removed order by order in perturbation theory. In contrast, the lattice is a non-perturbative cutoff. Before a calculation begins, all wavelengths less than a lattice spacing are removed.

All regulators have a price. On the lattice we sacrifice all continuous space-time symmetries but preserve all internal symmetries, including local gauge invariance. This preservation is important for non-perturbative physics. For example, gauge invariance is a property of the continuum theory which is non-perturbative, so maintaining it as we pass to the lattice means that all of its consequences (including current conservation and renormalizability) will be preserved. Of course, we want to make predictions for the real world, when all symmetries are present. It can be very expensive to recover the symmetries we lost by going on the lattice.

It is straightforward to construct the lattice version of a field theory. One just replaces the space-time coordinate x_μ by a set of integers n_μ ($x_\mu = an_\mu$, where a is the lattice spacing). Field variables $\phi(x)$ are defined on sites $\phi(x_n) \equiv \phi_n$. The action, an integral over the Lagrangian, is replaced by a sum over sites, and derivatives in the Lagrange density are replaced by finite differences.

$$S = \int d^4x \mathcal{L}(\phi(x)) \rightarrow a^4 \sum_n \mathcal{L}(\phi_n) \quad (1)$$

and the generating functional for Euclidean Green's functions is replaced by an ordinary integral over the lattice fields

$$Z = \int \left(\prod_n d\phi_n \right) e^S. \quad (2)$$

Gauge fields carry a space-time index μ in addition to an internal symmetry index a ($A_\mu^a(x)$) and are associated with a path in space $x_\mu(s)$: a particle traversing a

contour s in space picks up a phase factor

$$\psi \rightarrow P(\exp ig \int_s dx_\mu A_\mu) \psi \equiv U(s) \psi(x). \quad (3)$$

P is a path-ordering factor analogous to the time-ordering operator in ordinary quantum mechanics. Under a gauge transformation g , $U(s)$ is rotated at each end:

$$U(s) \rightarrow V(x_\mu(s)) U(s) V(x_\mu(0))^{-1}. \quad (4)$$

These considerations led Wilson² to formulate gauge fields on a space-time lattice, in terms of a set of fundamental variables which are elements of the gauge group G (I'll specialize to $SU(N)$ for N colors) living on the links of a four-dimensional lattice, connecting neighboring sites x and $x + a\mu$: $U_\mu(x)$,

$$U_\mu(x) = \exp(igaT^a A_\mu^a(x)) \quad (5)$$

(g is the coupling, A_μ the vector potential, and T^a is a group generator).

Under a gauge transformation link variables transform as

$$U_\mu(x) \rightarrow V(x) U_\mu(x) V(x + \hat{\mu})^\dagger \quad (6)$$

and site variables transform as

$$\psi(x) \rightarrow V(x) \psi(x). \quad (7)$$

We are usually only interested in gauge invariant observables. These will be either matter fields connected by oriented “strings” of U’s

$$\bar{\psi}(x_1) U_\mu(x_1) U_\mu(x_1 + \hat{\mu}) \dots \psi(x_2) \quad (8)$$

or closed oriented loops of U’s

$$\text{Tr} \dots U_\mu(x) U_\mu(x + \hat{\mu}) \dots \rightarrow \text{Tr} \dots U_\mu(x) V^\dagger(x + \hat{\mu}) V(x + \hat{\mu}) U_\mu(x + \hat{\mu}) \dots \quad (9)$$

An action is specified by recalling that the classical Yang-Mills action involves the curl of A_μ , $F_{\mu\nu}$. Thus a lattice action ought to involve a product of U_μ ’s around some closed contour. Gauge invariance will automatically be satisfied for actions built of powers of traces of U’s around arbitrary closed loops, with arbitrary coupling constants. If we assume that the gauge fields are smooth, we can expand the link variables in a power series in gaA'_μ ’s. For almost any closed loop, the leading term in the expansion will be proportional to $F_{\mu\nu}^2$. All lattice actions are just bare actions characterized by many bare parameters (coefficients of loops). In the continuum (scaling) limit all these actions are presumed to lie the same universality class, which is (presumably) the same universality class as QCD with any regularization scheme, and there will be cutoff-independent predictions from any lattice action which are simply predictions of QCD.

The simplest contour has a perimeter of four links. The “plaquette action” or “Wilson action” (after its inventor) is defined as

$$S = \frac{2}{g^2} \sum_n \sum_{\mu > \nu} \text{Re Tr} (1 - U_\mu(n) U_\nu(n + \hat{\mu}) U_\mu^\dagger(n + \hat{\nu}) U_\nu^\dagger(n)). \quad (10)$$

4 *DeGrand*

The bare lattice coupling, whose associated cutoff is a , is g^2 . The lattice parameter $\beta = 2N/g^2$ is often written instead of $g^2 = 4\pi\alpha_s$.

In the strong coupling limit, the lattice regularized version of a gauge theory with any internal symmetry group automatically confines². The interesting question is to understand what happens as the bare coupling became weaker at fixed lattice spacing (or for asymptotically free theories, what happens as the lattice spacing is taken to zero). In the strong coupling limit, chiral symmetry is also spontaneously broken³. While it is still not proved, all the evidence we have is that if the internal symmetry group is $SU(N)$, confinement and chiral symmetry persist as the lattice spacing is taken away.

2.2. Numerical Simulations

Lattice QCD has survived because it is a framework for doing “exact” (direct from a cutoff Lagrangian) calculations of QCD, which is simple enough in principle that it can be taught to a computer. In a lattice calculation, like any other calculation in quantum field theory, we compute an expectation value of any observable Γ as an average over an ensemble of field configurations:

$$\langle \Gamma \rangle = \frac{1}{Z} \int [d\phi] \exp(-S) \Gamma(\phi). \quad (11)$$

The average is done by numerical simulation: we construct an ensemble of states (collection of field variables), where the probability of finding a particular configuration in the ensemble is given by Boltzmann weighting (i. e. proportional to $\exp(-S)$). Then the expectation value of any observable Γ is given simply by an average over the ensemble:

$$\langle \Gamma \rangle \simeq \bar{\Gamma} \equiv \frac{1}{N} \sum_{i=1}^N \Gamma[\phi^{(i)}]. \quad (12)$$

As the number of measurements N becomes large the quantity $\bar{\Gamma}$ will become a Gaussian distribution about a mean value, our desired expectation value.

The idea of essentially all simulation algorithms⁴ is to construct a new configuration of field variables from an old one. One begins with some initial field configuration and monitors observables while the algorithm steps along. After some number of steps, the value of observables will appear to become independent of the starting configuration. At that point the system is said to be “in equilibrium” and Eq. 12 can be used to make measurements.

Dynamical fermions are a complication for QCD. The fermion path integral is not a number and a computer can’t simulate fermions directly. For n_f degenerate fermion flavors the generating functional for Green’s functions is

$$Z = \int [dU][d\psi][d\bar{\psi}] \exp(-\beta S_G(U) - \sum_{i=1}^{n_f} \bar{\psi} M(U) \psi) \quad (13)$$

One formally integrates out the fermions to give a pure gauge action where the probability measure includes a nonlocal interaction among the U 's:

$$Z = \int [dU] (\det M(U))^{n_f} \exp(-\beta S(U)) \quad (14)$$

or

$$Z = \int [dU] \exp(-\beta S(U) + n_f \text{Tr} \ln(M(U))). \quad (15)$$

Generating configurations of the U 's involves computing how the action changes when the set of U 's are varied. The presence of the determinant makes this problem very difficult. For a pure gauge theory, changing a variable at one location only affects the action at sites “near” the variable, so the attempt to update one link variable on the lattice involves a computational effort independent of the lattice volume (said differently, the cost of generating a new configuration scales with the lattice volume). However, the determinant is nonlocal, and so in principle updating one gauge variable would involve an amount of work proportional to the lattice volume.

Typically, this involves inverting the fermion matrix $M(U)$ (because the change in $\log M$ is $d \log M/dU = M^{-1} dM/dU$). This is the major computational problem dynamical fermion simulations face. M has eigenvalues with a very large range—from 2π down to $m_q a$. The “conditioning number” – the ratio of largest to smallest eigenvalue of the matrix – determines the convergence rate of iterative methods which invert it. In the physically interesting limit of small m_q the conditioning number diverges and the matrix is said to become “ill-conditioned.” The matrix becomes difficult (impossible) to invert. At present it is necessary to compute at unphysically heavy values of the quark mass and to extrapolate to $m_q = 0$. (The standard inversion technique today is one of the variants of the conjugate gradient algorithm.)

The tremendous expense of the determinant is responsible for one of the standard lattice approximations, the “quenched” approximation. In this approximation the back-reaction of the fermions on the gauge fields is neglected, by setting $n_f = 0$ in Eq. 13. Valence quarks, or quarks which appear in observables, are kept, but no sea quarks.

All large scale dynamical fermion simulations today generate configurations using some variation of the microcanonical ensemble. That is, they introduce momentum variables P conjugate to the U 's and integrate Hamilton's equations through a simulation time t

$$\dot{U} = iPU \quad (16)$$

$$\dot{P} = -\frac{\partial S_{eff}}{\partial U}. \quad (17)$$

The integration is done numerically by introducing a time step Δt . The momenta are repeatedly refreshed by bringing them in contact with a heat bath and the method is thus called Refreshed or Hybrid Molecular Dynamics⁵. The reason for

6 *DeGrand*

the use of these small time step algorithms is that for any change in any of the U 's, M^{-1} must be recomputed. When Eqn. 17 is integrated all of the U 's in the lattice are updated simultaneously, and only one matrix inversion is needed per change of all the bosonic variables.

For special values of n_f the equations of motion can be derived from a local Hamiltonian and in that case Δt systematics in the integration can be removed by an extra Metropolis accept/reject step. This method is called Hybrid Monte Carlo⁶. There are also many variations on these schemes⁷.

Recently, there has been a lot of exploration of alternative, large-step algorithms for dynamical fermions⁸. While these look promising, none has been used as much as the molecular dynamics methods.

2.3. Spectroscopy Calculations

Masses of hadrons are computed in lattice simulations from the asymptotic behavior of Euclidean-time correlation functions. A typical (diagonal) correlator can be written as

$$K(x) = \langle 0|O(x)O(0)|0\rangle. \quad (18)$$

This correlator has its Euclidean-space analog

$$\Pi(q) = \int d^4x \exp(iqx)K(x) \quad (19)$$

and if we assume that $\Pi(q)$ is dominated by a sum of resonances, we expect

$$\Pi(q) = \sum_n \frac{r_n}{q^2 + m_n^2} \quad (20)$$

where $r_n = |\langle 0|O|n\rangle|^2$. We can invert the Fourier transform to obtain a prediction for $K(x)$ (or some re-weighted analog). For example, lattice people often sum $K(x)$ over a three-dimensional volume of points ($x = \{t, \vec{r}\}$, sum \vec{r}) to produce

$$\begin{aligned} C(t) &= \sum_{\vec{r}} K(x) \\ &= \int \frac{dq_0}{2\pi} e^{iq_0 t} \sum_n \frac{r_n}{q_0^2 + m_n^2} \\ &= \sum_n \frac{r_n}{2m_n} e^{-m_n t} \end{aligned} \quad (21)$$

At large separation the correlation function is approximately

$$C(t) = \frac{r_1}{2m_1} e^{-m_1 t} \quad (22)$$

where m_1 is the mass of the lightest state which the operator O can create from the vacuum. Fig. 1 shows an example of a lattice correlator. Obviously, the lightest state in a channel is the easiest one to study. Excited states are hard to work with (their signal goes under the ground state's.) If the operator has vacuum quantum numbers

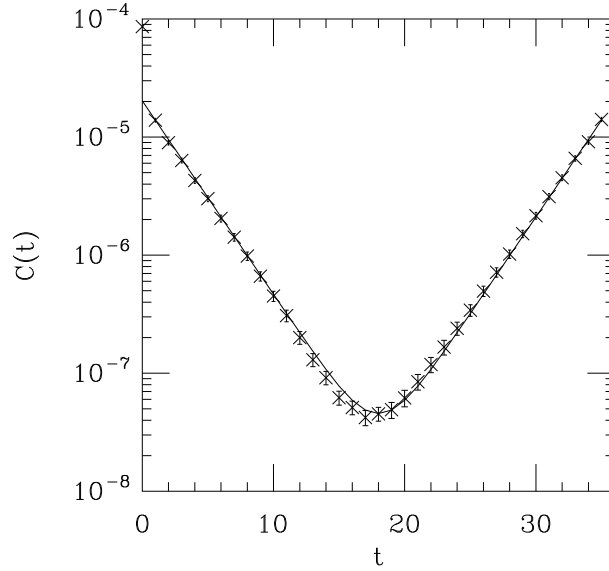


Fig. 1. A “better than typical” lattice correlator and its fit. Periodic boundary conditions convert the exponential decay into a hyperbolic cosine.

(an operator coupling to the scalar glueball is an example), the contribution for the “real” lightest state will disappear exponentially into the constant background. In that case it is also hard to measure a mass.

Most of the observables we are interested in will involve valence fermions. To compute the mass of a meson we might take

$$C(t) = \sum_x \langle J(x, t) J(0, 0) \rangle \quad (23)$$

where

$$J(x, t) = \bar{\psi}(x, t) \Gamma \psi(x, t) \quad (24)$$

and Γ is a Dirac matrix. The intermediate states $|n\rangle$ which saturate $C(x, t)$ are the hadrons which the current J can create from the vacuum: the pion, for a pseudoscalar current, the rho, for a vector current, and so on. Now we write out the correlator in terms of fermion fields

$$C(t) = \sum_x \langle 0 | \bar{\psi}_i^\alpha(x, t) \Gamma_{ij} \psi_j^\alpha(x, t) \bar{\psi}_k^\beta(0, 0) \Gamma_{kl} \psi_l^\beta(0, 0) | 0 \rangle \quad (25)$$

with a Roman index for spin and a Greek index for color. We contract creation and annihilation operators into quark propagators

$$\langle 0 | T(\psi_j^\alpha(x, t) \bar{\psi}_k^\beta(0, 0)) | 0 \rangle = G_{jk}^{\alpha\beta}(x, t; 0, 0) \quad (26)$$

so

$$C(t) = \sum_x \text{Tr} G(x, t; 0, 0) \Gamma G(0, 0; x, t) \Gamma \quad (27)$$

where the trace runs over spin and color indices. Baryons are constructed similarly.

In practice, lattice people do not use such simple operators for interpolating fields. Instead, they take more complicated operators which model the wave function of the meson. One way to do this would be to gauge fix the lattice to some smooth gauge, like Coulomb gauge, and take $O(\vec{x}_0, t) = \sum_{x,y} \bar{\psi}(x, t) \Gamma \psi(y, t) \Phi(x - x_0, y - x_0)$, where Φ is our guess for the wave function (I like Gaussians). These guesses often have parameters which can be “tuned” to enhance the signal. It’s important to note that the choice of trial function should not affect the measured mass, it just alters how quickly the leading term emerges from the sum.

2.4. *Getting rid of the lattice*

The lattice spacing a is unphysical: it was an UV cutoff we introduced by hand to regularize the theory. The couplings $\{g\}$ we typed into the computer were bare couplings which define the cutoff theory at cutoff scale a . When we take a to zero we must also specify how the couplings behave. The proper continuum limit comes when we take a to zero holding physical quantities fixed, not when we take a to zero at fixed lattice couplings $\{g\}$. (It’s conventional to think of a as a function of the bare couplings $\{g\}$, so people actually think about tuning the $\{g\}$ ’s to push a to zero. A lattice QCD action will have one marginally relevant coupling—the lattice analog of the gauge coupling – plus a set of coefficients of irrelevant operators. When they are present, quark masses are relevant operators, and they must also be tuned as the lattice spacing is varied. These quantities characterize the particular lattice discretization.)

On the lattice, if all quark masses are set to zero, the only dimensionful parameter is the lattice spacing, so all masses scale like $1/a$. Lattice Monte Carlo predictions are of dimensionless ratios of dimensionful quantities. One can determine the lattice spacing by fixing one mass from experiment, and then one can go on to predict any other dimensionful quantity. However, at nonzero lattice spacing, all predictions will depend on the lattice spacing. Imagine computing some masses at several values of the lattice spacing. (Pick several values of the bare parameters and calculate masses for each set of couplings.) If the lattice spacing is small enough, the typical behavior of a ratio will look like

$$(am_1(a))/(am_2(a)) = m_1(0)/m_2(0) + O(m_1a) + O((m_1a)^2) + \dots \quad (28)$$

(modulo powers of $\log(m_1a)$). The leading term does not depend on the value of the UV cutoff. That is our cutoff-independent prediction. Everything else is an artifact of the calculation. We say that a calculation “scales” if the a -dependent terms in Eq. 28 are zero or small enough that one can extrapolate to $a = 0$, and generically refer to all the a -dependent terms as “scale violations.” Clearly our engineering goal is to design our lattice simulation to minimize scale violations.

We can imagine expressing each dimensionless combination $am(a)$ as some function of the bare coupling(s) $\{g(a)\}$, $am = f(\{g(a)\})$. As $a \rightarrow 0$ we must tune the

set of couplings $\{g(a)\}$ so

$$\lim_{a \rightarrow 0} \frac{1}{a} f(\{g(a)\}) \rightarrow \text{constant}. \quad (29)$$

From the point of view of the lattice theory, we must tune $\{g\}$ so that correlation lengths $1/ma$ diverge. This will occur only at the locations of second (or higher) order phase transitions. In QCD the fixed point is $g_c = 0$ so we must tune the coupling to vanish as a goes to zero.

One needs to set the scale by taking one experimental number as input. A complication that you may not have thought of is that the theory we simulate on the computer might be different from the real world, so its spectrum would be different. For example, the quenched approximation, or for that matter QCD with two flavors of degenerate quarks, almost certainly does not have the same spectrum as QCD with six flavors of dynamical quarks with their appropriate masses. Using one mass to set the scale from one of these approximations to the real world might not give a prediction for another quantity which agrees with experiment.

2.5. Lattice Error Bars

Numbers presented from lattice simulations come with uncertainties. Phenomenologists ought to read carefully the parts of the papers which describe the error analysis, because there are many parts to a lattice number's uncertainty, all different. Some of the uncertainty is statistical: The sample of lattices is finite. Typically, the quoted statistical uncertainty includes uncertainty from a fit: it is rare that a simulation measures one global quantity which is the desired observable. Usually one has to take a lattice correlator, assume it has some functional form, and determine the parameters which characterize the shape of the curve. The fit function (eq. 22 is an example) may be only asymptotic, and one has to figure out what part of the data is described by one's function. A complication which enters in at this point is that different quantities measured on the same set of lattices are typically highly correlated. These correlations have to be taken into account in the fit.

Dimensionful quantities require (at least) two measurements: an additional quantity is needed to set the scale. Again, different quantities may be easier or harder to measure, so their lattice errors will vary. Clearly, people like to choose quantities which are as insensitive as possible to lattice artifacts, interpolation in mass, or other analysis issues. For example, one might want to use a hadron mass, or a decay constant, or a parameter associated with the heavy quark potential, to fix a . Many people use the rho mass, but perhaps this is not a good quantity: in the real world, the rho is unstable (and broad), so what will happen in a simulation? The S-P mass splitting in mesons is known to be relatively independent of the quark mass, but for light hadrons, the P-wave signal is noisy. Using heavy quark properties to fix the lattice spacing usually requires a different heavy quark action, with a separate simulation. There are endless arguments in the literature...

This is not the end of the analysis. It may be necessary to extrapolate or interpolate one's results to a particular value of the quark mass. One again needs a functional form. The fit or extrapolation has a statistical uncertainty, but now systematics begin to creep in: The functional dependence comes from some theory. Is the theory correct? Can it be applied to the whole range of quark masses where the lattice data exists?

Additional systematics arise in quenched approximation. Quenched QCD is not real-world QCD, and their spectra are presumably different. People publishing quenched numbers sometimes attempt to quote a systematic uncertainty from the quenched approximation. They might try to do this by using several different observables to set the lattice spacing, or to fix the quark mass, and seeing how the final result changes for different observables. The problem with this analysis is that it assumes that if the parameter values were chosen in the same way in quenched and full QCD (take the strange quark mass from the K^*/ϕ mass ratio, for example), the desired matrix element would also be the same in quenched and full QCD. There is no reason for that to be true. In full QCD there is supposed to be one unique value of the lattice spacing, so differences from different observables reflect on the quality of the simulation (assuming that QCD is in fact the correct description of Nature).

Finally, lattice quantities which are not spectral have scheme dependence. It is necessary to convert the lattice number to a number in some continuum regularization scheme. If this scheme matching is done nonperturbatively, the uncertainty in doing this is likely to be mostly statistical: the conversion factor comes from its own simulation. When the matching factor is computed in perturbation theory, most people will make "reasonable" choices for the way the calculation is organized (picking the scale at which the strong interaction coupling constant is determined, for example), vary their choices in some "reasonable" way, and attempt to assign an uncertainty based on the variation they see.

It is relatively easy to do simulations of gauge theories for any compact internal symmetry group, or any other bosonic system. Fermionic systems interacting with gauge or matter fields are feasible without enormous resources for fermion masses down to the strange quark mass, but become quite expensive below that value. Simulations with massless or nearly massless fermions remain at the costly frontier. Of course, large N_c simulations scale roughly like N_c^3 from the multiplication of the link matrices. In spectroscopy, properties of flavor non-singlet hadrons are easier to compute than those of flavor singlet ones (disconnected diagrams are noisy), and almost any calculation can be designed to scale linearly with the number of quark propagators which need to be strung together.

2.6. *Improvement: Why and How*

Today's QCD simulations range from $16^3 \times 32$ to $32^3 \times 100$ points and run from hundreds (quenched) to thousands (full QCD) of hours on the fastest supercom-

puters in the world. The cost of a Monte Carlo simulation in a box of physical size L with lattice spacing a and quark mass m_q scales roughly as

$$\left(\frac{L}{a}\right)^4 \left(\frac{1}{a}\right)^{1-2} \left(\frac{1}{m_q}\right)^{2-3} \quad (30)$$

where the first term in parentheses just counts the number of sites, the second term gives the cost of “critical slowing down”—the extent to which successive configurations are correlated, and the third term gives the cost of inverting the fermion propagator, plus critical slowing down from the nearly massless pions. Thus it is worthwhile to think about how to do the discretization, to maximize the value of the lattice spacing at which useful (scaling) simulations can be done.

Remember, the lattice action is just a bare action defined with a cutoff. No lattice discretization is any better or worse (in principle) than any other. Any bare action which is in the same universality class as QCD will produce universal numbers in the scaling limit. However, by clever engineering, it might be possible to devise actions whose scaling behavior is better, and which can be used at bigger lattice spacing.

To want to compute the value of some QCD observable via numerical simulation is to confront a daunting set of technical problems. The lattice volume must be large enough to contain the hadrons – and often, to allow them to be located far apart. High statistics are needed for reasonable accuracy. And the lattice spacing must be small enough to minimize discretization artifacts. These constraints push simulations onto large, fast, and often remote supercomputers. This introduces a new set of problems. These resources are expensive, so people form collaborations to share them. The fastest machines are the newest ones, which are often unstable, or hard to program, inefficient for all but restricted kinds of computations, or all of the above. Finally, because they are so big, lattice projects have a high profile. They cannot be allowed to fail.

Thus, until the late '90's, most simulations used the simplest discretizations, or minimal modifications to them. The last few years have seen a slow change in this situation, basically driven by necessity: standard methods become increasingly dominated by artifacts as the light quark masses become smaller and smaller. Two examples illustrate this.

First, groups doing dynamical fermion simulations with staggered fermions (see Sec. 3) want to do simulations with two nearly degenerate light quarks (the up and down quarks) and a heavier strange quark. With this kind of fermion, it is possible to do simulations with the strange quark mass at its physical value. However, staggered fermions suffer from flavor symmetry breaking (see Sec. 3.2), and at today's lattice spacings the standard formulation of staggered fermions produces a spectrum of mesons in which some of the non-strange pseudoscalars would be heavier than the strange ones. Then what is a pion, and what is a kaon? A more complicated discretization is needed to reduce the flavor symmetry breaking, so that the non-strange mesons are separated in mass from the strange ones.

12 *DeGrand*

A second example is the discovery of lattice discretizations with flavor symmetry and improved or exact chiral symmetry (domain wall and overlap fermions). Their extra computational expense is repaid by their ability to cleanly address problems (mostly involving chiral symmetry) the standard methods cannot.

The democratization of computing has helped. QCD is not yet possible on desk top machines, but a lot of interesting work can be done on clusters for a cost of a few tens of thousands of dollars.

(Of course, most people will still minimize the amount of evolution of their codes away from the well-studied algorithms because the original requirements of large volume and high statistics have not gone away.)

The simplest organizing principle for “improvement” is to use the canonical dimensionality of operators as a guide. Consider the gauge action as an example. If we perform a naive Taylor expansion of a lattice operator like the plaquette, we find that it can be written as

$$\begin{aligned}
 1 - \frac{1}{3}\text{Re Tr}U_{\text{plaq}} &= r_0\text{Tr}F_{\mu\nu}^2 + a^2[r_1\sum_{\mu\nu}\text{Tr}D_\mu F_{\nu\sigma}D_\mu F_{\nu\sigma} + \\
 &\quad r_2\sum_{\mu\nu\sigma}\text{Tr}D_\mu F_{\nu\sigma}D_\mu F_{\nu\sigma} + \\
 &\quad r_3\sum_{\mu\nu\sigma}\text{Tr}D_\mu F_{\mu\sigma}D_\nu F_{\nu\sigma}] + \\
 &\quad +O(a^4)
 \end{aligned} \tag{31}$$

The expansion coefficients have a power series expansion in the bare coupling, $r_j = A_j + g^2 B_j + \dots$. Other loops have a similar expansion, with different coefficients. The expectation value of any operator T computed using the plaquette action will have an expansion

$$\langle T(a) \rangle = \langle T(0) \rangle + O(a) + O(g^2 a) + \dots \tag{32}$$

Now the idea is to take the lattice action to be a minimal subset of loops and systematically remove the a^n terms for physical observables order by order in n by taking the right linear combination of loops in the action, $S = \sum_j c_j O_j$ with $c_j = c_j^0 + g^2 c_j^1 + \dots$. This method was developed by Symanzik and co-workers^{9,10,11} in the mid-80’s.

Renormalization group ideas have also been used to motivate improvement programs¹².

If you think about it, all the operators which are being added to the minimal discretizations are irrelevant operators. So in principle, no improvement method is really “wrong,” although it might happen that the cost of the improved action is greater than the gain from simulation fidelity. The final arbiter is a simulation. An example¹³ of a test of scale violations is shown in Fig. 2. The x axis is the lattice spacing, in units of a quantity r_1 , which is defined through the heavy quark potential: $r_1^2 dV(r)/dr|_{r_1} = 1.0$, about 0.4 fm. The plotting symbols are for different kinds of discretizations. The flatter the curve, the smaller the scale violations. The data labeled by squares shows the best scaling.

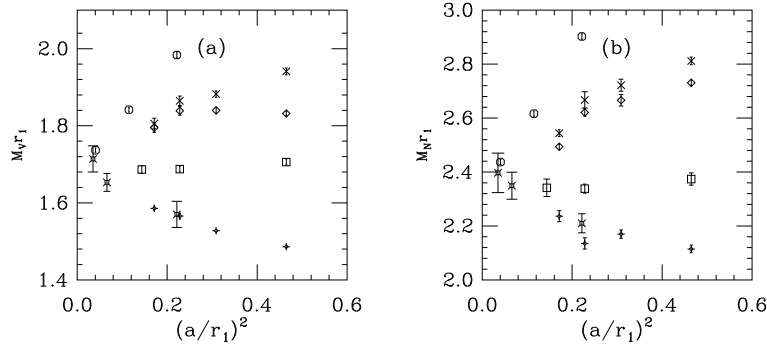


Fig. 2. Lattice calculations of the (a) rho and (b) nucleon mass, interpolated to the point $m_\pi r_1 = 0.778$, as a function of lattice spacing, from Ref. 13.

A recent innovation for improvement is the use of “fat links” as gauge connections in fermion actions. A standard “thin link” action has its gauge connections built out of a single link variable, $S \simeq \bar{\psi}(x)U_\mu(x)\psi(x+\hat{\mu})$. Fat links replace the single link by an average of paths. For example, a simple blocking (“APE blocking¹⁴”) is

$$\begin{aligned}
 V_\mu(x) = & (1 - \alpha)U_\mu(x) \\
 & + \alpha/6 \sum_{\nu \neq \mu} (U_\nu(x)U_\mu(x+\hat{\nu})U_\nu(x+\hat{\mu})^\dagger \\
 & + U_\nu(x-\hat{\nu})^\dagger U_\mu(x-\hat{\nu})U_\nu(x-\hat{\nu}+\hat{\mu})), \quad (33)
 \end{aligned}$$

with possibly a further projection back to the gauge group. The parameter α can be tuned. There are of course many possibilities. This year, the most popular choices for fattening include the Asqtad link¹⁵ (“ a^2 TADpole improved”) and the HYP (hypercubic) link¹⁶.

For smooth fields the fat links have an expansion $V_\mu(x) = 1 + iaB_\mu(x) + \dots$ and the original thin links have an expansion $U_\mu(x) = 1 + iaA_\mu(x) + \dots$, where

$$B_\mu(x) = \sum_{y,\nu} h_{\mu\nu}(y)A_\nu(x+y) \quad (34)$$

and the convolution function $h_{\mu\nu}(y)$ obviously depends on the fattening. Smoothing is easiest to see in momentum space, where the connection between the thin and fat link basically introduces a form factor¹⁷, $B_\mu(q) = \sum_\nu h_{\mu\nu}(q)A_\nu(q)$.

A number of ideas motivate fat links. They all boil down to the simple idea that a hard lattice cutoff introduces more discretization artifacts than a smoothed cutoff.

Clearly, the trade off is between smoothing the gauge field locally (at the cutoff scale) versus erasing physics at long distances. Fat links improve perturbation theory, reduce flavor symmetry breaking for staggered fermions, reduce chiral symmetry breaking for non-chiral discretizations, and help in the implementation of overlap actions¹⁸.

3. Relativistic Fermions on the Lattice

Finding a lattice discretization for light fermions involves yet another problem: doubling. Let's illustrate this with free field theory. The continuum free action is

$$S = \int d^4x [\bar{\psi}(x) \gamma_\mu \partial_\mu \psi(x) + m \bar{\psi}(x) \psi(x)]. \quad (35)$$

One obtains the so-called naive lattice formulation by replacing the derivatives by symmetric differences: we explicitly introduce the lattice spacing a in the denominator and write

$$S_L^{naive} = \sum_{n,\mu} \bar{\psi}_n \gamma_\mu \Delta_\mu \psi_n + m \sum_n \bar{\psi}_n \psi_n, \quad (36)$$

where the lattice derivative is

$$\Delta_\mu \psi_n = \frac{1}{2a} (\psi_{n+\mu} - \psi_{n-\mu}). \quad (37)$$

The propagator is easy to construct:

$$\frac{1}{a} G(p) = (i\gamma_\mu \sin p_\mu a + ma)^{-1} = \frac{-i\gamma_\mu \sin p_\mu a + ma}{\sum_\mu \sin^2 p_\mu a + m^2 a^2}. \quad (38)$$

Now the lattice momentum p_μ ranges from $-\pi/a$ to π/a . A continuum fermion with its propagator $(i\gamma_\mu p_\mu + m)^{-1}$ has a large contribution at small p from four modes which are bundled together into a single Dirac spinor. The lattice propagator has these modes too, at $p = (0, 0, 0, 0)$, but there are other degenerate ones, at $p = (\pi, 0, 0, 0)$, $(0, \pi, 0, 0)$, \dots (π, π, π, π) . As a goes to zero, the propagator is dominated by the places where the denominator is small, and there are sixteen of these (64 modes in all) in all the corners of the Brillouin zone. Thus our action is a model for sixteen light fermions, not one. This is the famous “doubling problem.”

The doubling problem is closely connected to the axial anomaly. Karsten and Smit¹⁹ showed by explicit calculations that the axial charges of the sixteen light fermions are paired and sum to zero. Many years ago Adler showed that it is not possible to find a continuum regulator which is gauge invariant for a theory with continuous chiral symmetry and a weak coupling limit with a perturbative expansion²⁰, and the lattice was not immune to this problem.

Nielsen and Ninomiya²¹ codified this constraint in a famous “no-go” theorem. In detail, the theorem assumes

- A quadratic fermion action $\bar{\psi}(x) H(x-y) \psi(y)$, where H is Hermitian, has a Fourier transform $H(p)$ defined for all p in the Brillouin zone, and has a continuous first derivative everywhere in the Brillouin zone. $H(p)$ should behave as $\gamma_\mu p_\mu$ for small p_μ .
- A local conserved charge Q defined as $Q = \sum_x j_0(x)$, where j_0 is a function of the field variables $\psi(y)$ where y is close to x .
- Q is quantized.

The statement of the theorem is that, once these conditions hold, $H(p)$ has an equal number of left handed and right handed fermions for each eigenvalue of Q .

There is a folkloric version of the theorem which says that no lattice action can be undoubled, chiral, and have couplings which extend over a finite number of lattice spacings (“ultra-locality”). This is actually not what the theorem says. It is the quantization of the charge which governs whether the theorem is evaded or not.

Ultra-locality is a historical engineering constraint on lattice action design. What is needed for a proper field theoretic description is locality, meaning that the range of the action is restricted to be on the order of the size of the spatial cutoff. It is believed that having lattice couplings which fall off exponentially with distance (measured in units of the lattice spacing), i.e. $S = \sum_{x,r} \bar{\psi}(x)C(r)\psi(x+r)$ with $C(r) \simeq \exp(-r/\xi)$, $\xi \propto a$, corresponds to a local action in the continuum limit, but that slower falloff (power law, for example) does not. Present day simulations have cutoffs of 0.2 to 0.05 fm, which is uncomfortably close to physical scales, and so people who work with non-ultra-local actions worry about the range of their actions, and try to tune them to maximize locality.

At the end of their paper, Nielsen and Ninomiya discuss ways to evade the theorem. They were not too optimistic about abandoning the quantization of charge, but that is how overlap and domain wall fermions achieve chirality.

Having said that, it is useful to classify lattice actions into their folkloric categories: ultra-local actions which are non-chiral and undoubled (Wilson fermions and their generalizations), ultra-local actions with quantized chiral charges, which are therefore doubled (staggered fermions), and chiral actions which evade the Nielsen-Ninomiya theorem, the related cases of domain wall and overlap fermions.

3.1. Wilson Fermions (undoubled, non-chiral, ultra-local)

We can alter the dispersion relation so that it has only one low energy solution. The other solutions are forced to $E \simeq 1/a$ and become very heavy as a is taken to zero. The simplest version of this solution, called a Wilson fermion, adds an irrelevant operator, a second-derivative-like term

$$S^W = -\frac{r}{2a} \sum_{n,\mu} \bar{\psi}_n (\psi_{n+\mu} - 2\psi_n + \psi_{n-\mu}) \simeq ar\bar{\psi}D^2\psi \quad (39)$$

to S^{naive} . The parameter $r = 1$ is almost always used and is implied when one speaks of using “Wilson fermions.” The propagator is

$$\frac{1}{a}G(p) = \frac{-i\gamma_\mu \sin p_\mu a + ma - r \sum_\mu (\cos p_\mu a - 1)}{\sum_\mu \sin^2 p_\mu a + (ma - r \sum_\mu (\cos p_\mu a - 1))^2}. \quad (40)$$

It remains large at $p_\mu \simeq (0, 0, 0, 0)$, but the “doubler modes” are lifted at any fixed nonzero r so $G(p)^{-1}$ has one four-component minimum.

There are actually two dimension-five operators which can be added to a fermion action. The Wilson term is just one of them. The other dimension-five term is a

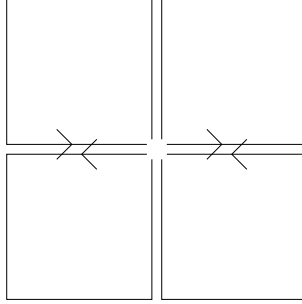


Fig. 3. The “clover term”.

magnetic moment term

$$S_{SW} - \frac{ia g}{4} \bar{\psi}(x) \sigma_{\mu\nu} F_{\mu\nu} \psi(x) \quad (41)$$

and if both terms are included, their coefficients can be tuned so that there are no $O(a)$ or $O(ag^2)$ lattice artifacts. This action is called the “Sheikholeslami-Wohlert²²” or “clover” action because the lattice version of $F_{\mu\nu}$ (we’ll call it $C_{\mu\nu}$ below) is the sum of imaginary parts of the product of links around the paths shown in Fig. 3. These days, pure Wilson fermions are rarely used, having been replaced by the clover action (with various choices of clover term).

With Wilson fermions it is conventional to talk about “hopping parameter” $\kappa = \frac{1}{2}(ma + 4r)^{-1}$, and to rescale the fields $\psi \rightarrow \sqrt{2\kappa}\psi$. The action for an interacting theory is conventionally written

$$S = \sum_n \bar{\psi}_n \psi_n - \kappa \sum_{n\mu} (\bar{\psi}_n(r - \gamma_\mu) U_\mu(n) \psi_{n+\mu} + \bar{\psi}_n(r + \gamma_\mu) U_\mu^\dagger \psi_{n-\mu}) + c_{SW} \bar{\psi}(x) \sigma_{\mu\nu} C_{\mu\nu} \psi(x). \quad (42)$$

$$(43)$$

From an operational point of view, Wilson-type fermions are closest to the continuum formulation—there is a four component spinor on every lattice site for every color and/or flavor of quark. The simplest bilinears $(\bar{\psi}(x) \gamma_\mu \psi(x))$, for example, could be used as interpolating fields, although in practice more complicated constructs are used to remove lattice artifacts from simulation results.

Wilson-type fermions contain explicit chiral-symmetry breaking terms. This is a source of many bad lattice artifacts. The most obvious is that the zero bare quark mass limit is not respected by interactions; the quark mass is additively renormalized. The value of bare quark mass m_q which the pion mass vanishes, is not known a priori before beginning a simulation. It must be computed. Simulations with Wilson fermions have to map out m_π vs am_q by direct observation. A second serious problem with the loss of chiral symmetry breaking is the mixing of operators which would not mix in the continuum. This compromises matrix element calculations. (See Sec. 6.2 for more discussion.) Finally, nothing prevents the Wilson-Dirac operator on a gauge configuration from developing a real eigenmode λ at any value. If

$-\lambda$ happened to equal the bare quark mass dialed into the program, $D + m$ would be non-invertible. In practice, these “exceptional configurations” make it difficult (if not impossible) to push to small values of the quark mass with non-chiral fermions. Rare indeed is the Wilson or clover calculation done at pseudoscalar-to-vector mass ratio much below 0.6.

Besides the simple actions I have described, there are Baroque variations which are designed to improve either the kinetic properties (dispersion relation), or chiral properties (minimize additive mass renormalization), or both²³.

A recent development²⁴ which removes exceptional configurations is “twisted mass QCD.” This is a scheme for $N_f = 2$ flavors in which the lattice Dirac operator is expanded to be

$$D_{twist} = D_W + i\mu\gamma_5\tau_3. \quad (44)$$

The isospin generator τ_3 acts in flavor space. The extra term is called the “chirally twisted mass.” It protects the Dirac operator against exceptional configurations for any finite μ : $\det D_{twist} = \det(D_W^\dagger D_W + \mu^2)$. It is an amusing exercise to use the axial transformations $\psi \rightarrow \exp(i\alpha\tau_3\gamma_5)$, $\bar{\psi} \rightarrow \bar{\psi}\exp(i\alpha\tau_3\gamma_5)$ to disentangle what would otherwise appear to be an unfortunate mixing of opposite-parity operators. I am aware of quenched calculations with this action²⁵, but so far, there are no published full QCD simulations.

3.2. Staggered or Kogut-Susskind Fermions (chiral, doubled, ultra-local)

The sixteen-fold degeneracy doublers of naive fermions can be condensed to four by the local transformation $\psi_n \rightarrow \Omega_n\chi_n$, $\bar{\psi}_n \rightarrow \bar{\chi}_n\Omega_n^\dagger$ where

$$\Omega_n = \prod_{\mu=0}^3 (\gamma_\mu)^{n_\mu}. \quad (45)$$

There are sixteen different Ω 's. Using

$$\begin{aligned} \Omega_n^\dagger\Omega_n &= 1; \\ \Omega_n^\dagger\gamma_\mu\Omega_{n+\hat{\mu}} &= (-1)^{n_0+n_1+\dots+n_{\mu-1}} \equiv \alpha_\mu(n), \end{aligned} \quad (46)$$

we rewrite the action as

$$S = \sum_n \bar{\psi}_n(\gamma_\mu \cdot \Delta_\mu + m)\psi_n = \sum_n \bar{\chi}_n(\alpha(n) \cdot \Delta + m)\chi_n. \quad (47)$$

Written in terms of χ , the action is diagonal in spinor space. Although we did the derivation for free-field theory, it is true for any background gauge field. χ is a four-component spinor, but since all components interact independently and identically, we can reduce the multiplicity of naive fermions by a factor of four simply by discarding all but one Dirac component of χ . These are “staggered fermions.”

18 *DeGrand*

It is natural to think of the 16 components of a staggered fermion as a fourfold replication of four Dirac components. The replication is called “taste.” “Taste” is the modern word for what used to be called “flavor,” as in the sentence “a single staggered fermion corresponds to four flavors/tastes.”

There are (at least) two ways to think about the taste content of free staggered fermions. The simplest is just to work in momentum space and break up the lattice Brillouin zone into 16 components, labeling $s_\mu = 0, 1$ for each direction, with a reduced zone for each component (the “central” one is $-\pi/(2a) < p_\mu(s) < \pi/(2a)$). The massless action is

$$S \simeq \sum_s \int_{p_s} \bar{\psi}(-p) \sum_\mu i\gamma_\mu \sin(p_\mu) \psi(p) \quad (48)$$

The “hypercubic” decomposition is used in simulations. Break the lattice up into 2^4 site hypercubes and bundle the fields in the hypercube together. Now we define the first and second block derivatives ($b = 2a$) by

$$\Delta_\mu \chi_n(N) = \frac{1}{2b} (\chi_n(N + \hat{\mu}) - \chi_n(N - \hat{\mu})) \quad (49)$$

$$\square_\mu \chi_n(N) = \frac{\chi_n(N + \hat{\mu}) + \chi_n(N - \hat{\mu}) - 2\chi_n(N)}{b^2} \quad (50)$$

In this basis the action is

$$S \simeq \sum_{x,\mu} b^4 \bar{\psi}(x) \left[(\gamma_\mu \otimes I) \Delta_\mu + \frac{1}{2} b (\gamma_5 \otimes \gamma_\mu^* \gamma_5) \square_\mu \right] \psi(x) + mb^4 \sum_x \bar{\psi}(x) I \otimes I \psi(x) \quad (51)$$

The sum over $x (= Nb)$ runs over all hypercubes of the blocked lattice. (The notation is (spin \otimes taste). Taste symmetry is four-fold, so the use of Dirac matrices for its generators is natural.) The presence of the $(\gamma_5 \otimes \gamma_\mu^* \gamma_5)$ term shows that the hypercube decomposition still has flavor mixing away from the $a \rightarrow 0$ limit.

In the continuum, QCD with four degenerate massless flavors has an $SU(4)_L \otimes SU(4)_R \otimes U(1)_V$ symmetry, which spontaneously breaks to $SU(4)_V$, and the pseudoscalar spectrum consists of 15 Goldstone particles and a massive (from the anomaly) eta-prime. On the lattice, taste and spin rotations are replaced by shifts and rotations in the hypercube. The continuous symmetries of the continuum are broken down to discrete symmetries. In particular, taste symmetry is broken. Only a $U(1)_V \otimes U(1)_A$ survives, and the spontaneous breaking of the lattice analog of the flavor non-singlet axial symmetry produces a single Goldstone boson at nonzero a . The other “would-be” Goldstones are non-degenerate pseudoscalar states whose mass goes to zero in the continuum limit. (QCD with N_f flavors of staggered fermions has an internal $SU(N_f)_L \otimes SU(N_f)_R$ chiral symmetry.) The $U(1)$ chiral symmetry protects the quark mass from additive renormalization, and staggered fermions are preferred over Wilson ones in situations in which the chiral properties of the fermions dominate the dynamics.

There are two complementary ways to think about taste breaking. In momentum space, taste mixing occurs in perturbation theory via the emission and absorption of

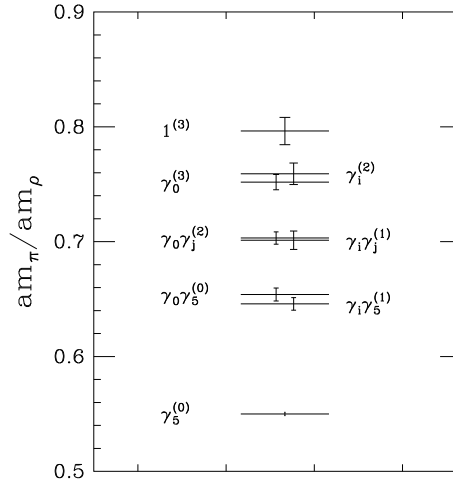


Fig. 4. An example of flavor symmetry breaking in an improved staggered action. The different γ 's are a code for the various pseudoscalar states. Data are from Ref. 15. For an explanation of the splitting, see Ref. 26.

gluons with momentum near $q_\mu = \pi/a$. These kick quarks from one s_μ momentum sector into another one. In the hypercube basis, different tastes sit on different locations in the hypercube. The environment of link variables varies across the hypercube, so different tastes see different local gauge fields.

The pseudoscalar spectrum shows an interesting (approximate) degeneracy (see Fig. 4 for an example), first described by Sharpe and Lee²⁶. It is reminiscent of the pattern of splittings of the energy levels of an atom in a crystal lattice.

Today's approach to staggered fermion simulations exploits the conversion of a $U(1)$ chiral symmetry for a single staggered flavor (with its single would be Goldstone boson) into the $SU(N_f)$ chiral symmetry of N_f flavors (with $N_f^2 - 1$ Goldstones). QCD with three flavors of quarks is treated with a lattice model with three flavors of staggered fermions, each with its own mass. Each flavor would correspond to four tastes. Three of the four tastes (per flavor) have to be excised from one's predictions. How that is done is different for valence and sea quarks, and will be described below.

This decomposition has been around since the mid-90's^{27,28}. It was introduced in order to understand weak matrix elements of staggered fermions. Recent techniques for staggered fermions, which make heavy use of chiral Lagrangians, have brought it to greater importance.

Taste symmetry violation for a single staggered flavor basically means that interactions mix the different tastes. For the connection between staggered flavor and physical flavor to work, taste symmetry violation must be minimized. People attack this problem in two ways.

20 *DeGrand*

First, they modify the action to suppress taste violations. This is commonly done by replacing the thin links of the fermion connection by a fat link. The “Asqtad” fat link action¹⁵ (which also adds a third - nearest - neighbor coupling to improve the dispersion relation) has seen the most extensive use. Other choices¹⁶ reduce taste violations more.

Second, lattice data is analyzed including the effects of taste violations. The key to doing this was provided by the Sharpe and Lee²⁶ analysis of taste mixing, whose construction of a low energy chiral effective theory including explicit taste-breaking interactions predicted the degeneracies shown in Fig. 4. Their work was generalized by Aubin and Bernard²⁹ to N_f flavors of staggered fermions ($4N_f$ tastes). One introduces a field $\Sigma = \exp(i\Phi/f)$, a $4N_f \times 4N_f$ matrix, and Φ is given by:

$$\Phi = \begin{pmatrix} U & \pi^+ & K^+ & \cdots \\ \pi^- & D & K^0 & \cdots \\ K^- & \bar{K}^0 & S & \cdots \\ \vdots & \vdots & \vdots & \ddots \end{pmatrix}, \quad (52)$$

The entries are the meson fields composed of different staggered flavors, and are traces over the 16 taste-product $q\bar{q}$ bilinears of each staggered flavor. The mass matrix is

$$\mathcal{M} = \begin{pmatrix} m_u I & 0 & 0 & \cdots \\ 0 & m_d I & 0 & \cdots \\ 0 & 0 & m_s I & \cdots \\ \vdots & \vdots & \vdots & \ddots \end{pmatrix}, \quad (53)$$

The Lagrangian is

$$\mathcal{L} = \frac{f^2}{8} \text{Tr}(\partial_\mu \Sigma \partial_\mu \Sigma^\dagger) - \frac{1}{4} \mu f^2 \text{Tr}(\mathcal{M} \Sigma + \mathcal{M} \Sigma^\dagger) \quad (54)$$

$$+ \frac{2m_0^2}{3} (U_I + D_I + S_I + \cdots)^2 + a^2 \mathcal{V}, \quad (55)$$

where the m_0^2 term weighs the analog of the flavor singlet η' . (The “ I ” subscripts display that this involves the taste singlet term for each flavor.) The $a^2 \mathcal{V}$ term is the taste-breaking interaction, a sum of terms quadratic in Σ with various taste projectors, parameterized by six coefficients (only one is big). Now one computes “any” desired quantity with this Lagrangian, typically to one loop, as a function of quark masses and all other coefficients. Parameters of Nature are determined when mass-dependent Monte Carlo data is fit to this functional form. For example, a one-loop fit to $m_{PS}/(m_1 + m_2)$ for the true would-be Goldstone boson made of quarks of mass m_1 and m_2 would involve μ , f , two Gasser-Leutwyler parameters, three otherwise unconstrained lattice parameters, and involves chiral logarithms whose arguments are all the observed pseudoscalar masses. Fits to f_π or f_K are similar.

It is crucial to analyze staggered data this way. In 2001 the MILC collaboration tried and failed to fit their pseudoscalar masses to the continuum chiral logarithm formula. The same data, with fits which include taste violations, forms part of their recent high precision calculation of hadronic parameters (see Sec. 5).

3.3. *Evading the no-go theorem – domain wall and overlap fermions*

Two related schemes allow one to evade the Nielsen-Ninomiya theorem. The first action is the “domain wall fermion^{30,31}.” It is a variation on the idea that a fermion coupled to a scalar field which interpolates between two minima (a soliton) will develop a zero-energy chiral mode bound to the center of the soliton. Embed QCD in a five-dimensional brane world with a kink. This is a discretized fifth dimension. The gauge fields remain four dimensional. A chiral fermion will sit on the four dimensional face of the kink. This is the chiral “domain wall fermion.” As Kaplan puts it, “The extra dimension is the loophole in the Nielsen-Ninomiya theorem through which the fermions have wriggled.”

Several groups have well-developed programs of QCD phenomenology, both quenched and dynamical, with domain wall fermions³². We will encounter their results in the section of this review dealing with kaon physics.

The practical consideration which must be dealt with in domain wall simulations is that in the computer, the fifth dimension is not infinite. There will be an anti-kink somewhere else in the fifth dimension or some equivalent boundary surface, with an opposite-chirality fermion pinned to it. As long as the two kinks are far away, the fermionic chiral mode on the kink doesn’t see the mode on the anti-kink and the 4-d theory on the kink will remain chiral. But if the anti-kink is too close (typically, if the fifth dimension is too small or the fermion eigenmodes on the kink are insufficiently localized in the fifth dimension) the modes mix and chiral symmetry is broken. The fermion will be observed to pick up a small additive mass renormalization. How close is “too close” is (yet) another engineering question, and is dealt with in the usual way (by modifying lattice discretizations).

The four-dimensional analog of this formulation uses the Ginsparg-Wilson relation³³

$$\gamma_5 D(0) + D(0)\gamma_5 = \frac{1}{2x_0} D(0)\gamma_5 D(0). \quad (56)$$

Its explicit realization is Neuberger’s “overlap fermion³⁴.” The massless overlap Dirac operator is

$$D(0) = x_0 \left(1 + \frac{z}{\sqrt{z^\dagger z}} \right) \quad (57)$$

where $z = d(-x_0)/x_0 = (d - x_0)/x_0$ and $d(m) = d + m$ is a massive “kernel” Dirac operator for mass m . d can be (almost) any undoubled lattice Dirac operator. The

22 *DeGrand*

chiral symmetry of these remarkable actions prevents additive mass renormalization, preserves all continuum Ward identities (up to contact terms) and knows about the index theorem³⁵.

The eigenmodes of $D(0)$ sit on a circle of radius x_0 centered at $(x_0, 0)$ in the complex plane. The zero mode is chiral (as is the mode at $(2x_0, 0)$) and the complex modes are non-chiral and paired (with complex conjugate eigenvalues). The Nielsen-Ninimiya theorem is evaded because the chiral charges are not quantized. One way³⁶ to see this is to realize that the action $S = \bar{\psi}D(0)\psi$ is invariant under the gauge field dependent axial transformation³⁷

$$\delta\psi = T\hat{\gamma}_5\psi = T\gamma_5\left(1 - \frac{D}{x_0}\right)\psi; \quad \delta\bar{\psi} = \bar{\psi}\gamma_5T \quad (58)$$

where T is a $U(N_f)$ flavor rotation generator. Directly from the Ginsparg-Wilson relation, $(\hat{\gamma}_5)^2 = 1$, so the combination of this axial vector transformation, plus the usual vector one, generates a conventional current algebra. The fermion measure is not invariant under the $U(1)_A$ version of Eq. 58, and this leads to the anomaly. For small D , Eq. 58 is the usual chiral rotation. This is the situation for the low eigenmodes of the Dirac operator. But at the other corners of the Brillouin zone $D \simeq 2x_0$, $\hat{\gamma}_5$ flips sign, and the transformation does not correspond to a chiral rotation. One can also consider a symmetric version of Eq. 58:

$$\delta\psi = T\gamma_5\left(1 - \frac{D}{2x_0}\right)\psi; \quad \delta\bar{\psi} = \bar{\psi}\left(1 - \frac{D}{2x_0}\right)T\gamma_5 \quad (59)$$

At the “far corners” of the Brillouin zone, where $D = 2x_0$, this transformation vanishes. Either way, the eigenvalue of the chiral charge is not quantized, it varies with D .

The massive overlap Dirac operator is conventionally defined to be

$$D(m_q) = \left(1 - \frac{m_q}{2x_0}\right)D(0) + m_q \quad (60)$$

and it is also conventional to define the propagator so that the chiral modes at $\lambda = 2x_0$ are projected out,

$$\hat{D}^{-1}(m_q) = \frac{1}{1 - m_q/(2x_0)}\left(D^{-1}(m_q) - \frac{1}{2x_0}\right). \quad (61)$$

This also converts local currents into order a^2 improved operators³⁸.

No overlap action is ultra-local³⁹. Satisfying the Ginsparg-Wilson relation requires an action which has connections spread out to an arbitrary number of lattice spacings. For sufficiently smooth gauge configurations, Hernandez, Jansen, and Luscher have proved that overlap actions are local⁴⁰. Golterman and Shamir⁴¹ have presented a convincing argument that sufficiently rough gauge configurations can drive overlap and domain wall fermion actions nonlocal. It is presently an item of debate, how much today’s simulations are corrupted by non-locality.

The hard part of an overlap calculation is the “step function” ($\epsilon(z) = \gamma_5 z / \sqrt{z^\dagger z}$). There are various tricks for evaluating it, basically as polynomials in z (Chebyshev

polynomials) or as a ratio of polynomials $A(z)/B(z) \simeq \gamma_5 z \sum (1/(z^\dagger z + c_n))$. (For discussions of overlap technology, see Refs. 42, 43.) The degree of success of these evaluations typically depends on the conditioning number of z , and to improve that, people remove low eigenmodes of z from the evaluation and treat them exactly. Overlap calculations typically cost a factor of 50-100 as much as ordinary Wilson calculations, but to quote that fact alone is unfair: they can be used to study small quark mass (chiral) physics with full flavor symmetry at quark masses where Wilson-type actions simply fail due to exceptional configurations. Unfortunately, overlap fermions are still too expensive for anything but extremely tentative dynamical fermion simulations.

There is of course an aesthetic (or engineering) debate among lattice practitioners over whether it is better to do simulations which have approximate chiral symmetry or exact chiral symmetry. The former are generally computationally less expensive, but they have to be checked against the appearance of unwanted effects. With an exact algorithm, one might sleep better at night knowing that the calculation does not have chiral artifacts, but it might also happen that one is simply unable to generate an interesting data set for analysis.

Because simulations with domain wall and overlap fermions are so expensive, there is a tendency to cut corners, either by making the lattice spacing uncomfortably large, or the simulation volume too small. (The author's calculation of B_K using overlap fermions is done at a small enough volume, that baryon masses are clearly affected—they are pushed to artificially high mass by the squeezing of the box.)

One can turn a bug into a feature by simulating QCD in the “epsilon regime”⁴⁴. This is QCD in a box whose length L is small compared to the pion Compton wavelength, $m_\pi L \ll 1$. It is not small simulation volume, since L should also be large compared to any “typical” QCD confinement scale. This year we have begun to see simulations (mostly with overlap fermions) in this regime⁴⁵. By analyzing the behavior of hadron correlators, and matching onto chiral Lagrangian calculations, also done in the epsilon regime, low energy properties of QCD may be extracted.

The descriptions of domain wall and overlap fermions did not make them look particularly similar. The connection comes when one takes domain wall fermions and integrates out the bulk fields to construct a four dimensional effective action of the light “pinned” fields^{34,46},

$$D = 1 + \gamma_5 \frac{(1+H)^{N_5} - (1-H)^{N_5}}{(1+H)^{N_5} + (1-H)^{N_5}} \quad (62)$$

where $H = \gamma_5 z / (2+z)$ and z was defined above. As the length of the fifth dimension becomes infinite and the lattice spacing in the fifth dimension vanishes, this Dirac operator becomes the overlap operator.

Finally, different kinds of fermions have different constraints on the number of flavors which can be simulated with various algorithms. Consider a single flavor of staggered (four tastes) or Wilson-type fermions (one flavor), with a massive Dirac

operator M . In either case $M^\dagger = \gamma_5 M \gamma_5$. The functional integral for a theory with a single flavor is just $\det M$. The massless staggered fermion Dirac operator $M(m=0)$ is antihermitian so its eigenvalues lie along the imaginary axis, and they come in pairs $\pm i\lambda$. For massive fermions, $\det M$ is a product of $(i\lambda + m)(-i\lambda + m)$ factors, thus it is positive-definite for all gauge configurations. Standard algorithms (Refreshed Molecular Dynamics⁵, Hybrid Monte Carlo⁶) actually work with $M^\dagger M$, which would redouble the number of flavors. But because $M^\dagger M$ only connects “even” sites on the lattice with other “even” sites (and “odd” with “odd”), one can take the square root of the operator by removing the fermion fields on all the “even” (or “odd”) sites.

Wilson fermions have eigenvalues which are real, and complex conjugate pairs. The determinant from the complex conjugate pairs is basically just like the staggered determinant; it is a product of $(m + \lambda_r)^2 + \lambda_i^2$. This part is positive definite. However, nothing protects the real eigenvalues from taking any value, so the product of real eigenvalues could have any sign, and could change sign as the gauge field evolves. With two degenerate flavors (or $N_f = 2j$), one can get a positive determinant because $\det M = \det M^\dagger$ and $(\det M)^2 = \det(M^\dagger M)$.

Furman and Shamir³¹ have proved that one can simulate any number of flavors with domain wall fermions. For overlap fermions, the real eigenvalues are restricted to be either zero or a positive number, and so one could also simulate any number of fermions, each one with its own $\det M$, with no problem with positivity⁴⁷.

4. The Quenched Approximation in Health and Sickness

For many years, calculations of spectroscopy and matrix elements in QCD have used the “quenched approximation” in which the fermion determinant is completely discarded from the functional integral. This approximation was adopted pretty much for reasons of expediency, because numerical simulations in full QCD were simply too expensive. From its earliest days it has produced results for known quantities which were in remarkable agreement with experiment. The results of one very careful quenched simulation⁴⁸ of the light hadron spectrum are shown in Fig. 5. One could not ask for anything better.

The quenched approximation has many of the ingredients of successful hadron phenomenology. Quarks are confined (with a linear confining potential if they are heavy). Chiral symmetry is spontaneously broken. In it, all states are (at first glance) infinitely narrow, because $q\bar{q}$ pairs cannot pop out of the vacuum. One might also try to “justify” the quenched approximation by an appeal to the quark model: in the quenched approximation, all mesons are $q\bar{q}$ pairs, and all baryons are qqq states. This also appears to be rather similar to the large- N_c limit of QCD.

However, the situation has changed. For about ten years people have identified specific situations where the quenched approximation would give qualitatively different behavior than QCD with any nonzero number of sea quarks. This behavior now needs to be dealt with – or is beginning to be seen – in simulations.

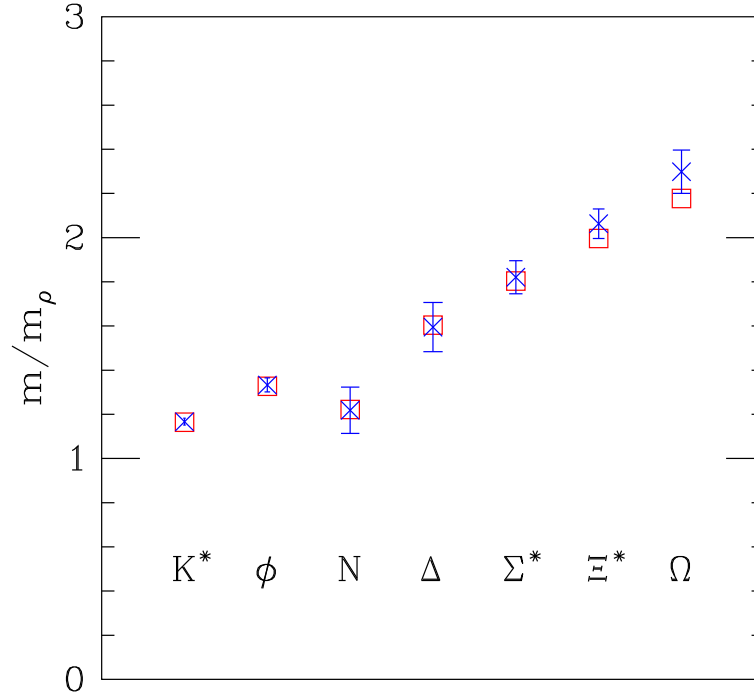


Fig. 5. Comparison of quenched results from Ref. 48 with experiment.

The best way to see what is going on is to consider the low energy limit of QCD, and not to think about quarks and gluons, but in terms of an effective field theory theory of QCD, described by chiral Lagrangians in which the would-be Goldstone bosons are fundamental fields. These Lagrangians have a set of bare parameters (quark masses, f_π , the quark condensate Σ , ...). As far as the chiral Lagrangian is concerned, these are fundamental parameters. As far as QCD is concerned, one could compute these parameters from first principles (for example, $f_\pi m_\pi = \langle 0 | \bar{\psi} \gamma_0 \gamma_5 \psi | \pi \rangle$), this would fix the parameters of the chiral Lagrangian, and then one could throw away the lattice and compute low energy physics using the chiral Lagrangian. Quenched QCD and QCD with nonzero flavor numbers are different theories and their low energy parameters will be different. But there is more. In full QCD the eta prime is heavy and can be decoupled from the interactions of the ordinary Goldstone bosons. In quenched QCD the eta prime is not really a particle. The would-be eta prime gives rise to “hairpin insertions” which pollute essentially all predictions.

Let’s consider the eta prime channel in full QCD and quenched QCD in various extreme limits. In ordinary QCD, the eta prime propagator includes a series of terms in which the flavor singlet $q\bar{q}$ pair annihilates into some quarkless state, then reappears, over and over. This is shown in Fig. 6. Let’s assume we have N_v valence quarks, N_s sea quarks, and N_c colors. (The case $N_v \neq N_s$ with $N_s \neq 0$ is called

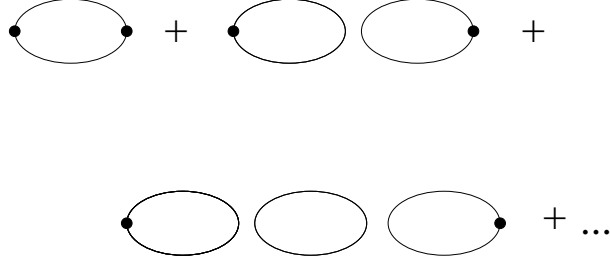
26 *DeGrand*


Fig. 6. The eta-prime propagator in terms of a set of annihilation graphs summing into a geometric series to shift the eta-prime mass away from the mass of the flavor non-singlet pseudoscalar mesons. In the quenched approximation, only the first two terms in the series survive as the “direct” and “hairpin” graphs.

“partial quenching” as opposed to the $N_s = 0$ quenched approximation.) Let’s sum the geometric series for the eta prime propagator

$$\eta'(q) = C(q) - H_0(q) + H_1(q) + \dots \quad (63)$$

where $C(q) = 1/d$, $d = q^2 + m_\pi^2$, is the “connected” meson propagator, the same as for any other Goldstone boson. H_n is the n th order hairpin (with n internal fermion loops). Simple N_c counting appropriate to the large- N_c limit (taking $g^2 N_c$ fixed), with flavor and color singlet sources and sinks, shows that $C(q) \propto N_c^0 N_V^0$ and $H_n(q) \propto 1/N_c^n$.

The lowest order hairpin is

$$H_0(q) = \frac{1}{d} \frac{N_v}{N_c} \lambda^2 \frac{1}{d} \quad (64)$$

where λ^2 is $O(N_c^0)$. Each extra loop gives another factor of $-N_s \lambda^2 / (N_c d)$. Summing the geometric series, we find

$$\eta'(q) = \frac{1}{d} \left(1 - \frac{N_v}{N_s}\right) + \frac{N_v}{N_s} \frac{1}{d + \lambda^2 N_s / N_c}. \quad (65)$$

This formula has a number of interesting limits. First, if $N_v = N_s = N_f \neq 0$, we see that we have generated a massive η' propagator with $m_{\eta'}^2 = \lambda^2 N_f / N_c$.

The next case is $N_v < N_s$. There we have both the Goldstone mode and the eta prime propagator. This is also as expected: think of the $SU(3)$ flavor symmetry limit and imagine a source $\bar{u}u + \bar{d}d$: it couples to a mixture of the eta (a Goldstone) and the eta prime.

Now we could take N_c to infinity at fixed N_f . With N_c -scaling of the vertex, the eta-prime mass falls to zero, and it becomes a ninth Goldstone boson as $U(1)_A$ is restored. At any finite N_c , the eta prime is still an ordinary particle.

However, the quenched limit is different—it is $N_s = 0$ first. In that case (of course)

$$\eta'(q) = \frac{1}{d} - \frac{1}{d} \frac{N_v}{N_c} \lambda^2 \frac{1}{d}, \quad (66)$$

In the eta prime channel there is an ordinary (but flavor singlet) Goldstone boson and a new contribution—a double-pole ghost (negative norm) state. In the $N_c = \infty$ limit, the double pole decouples, but finite N_c quenched QCD remains different from finite- N_c full QCD. The limits of large N_c and quenching don't commute.

Similar behavior will occur in any other flavor singlet channel (think about the ω meson), of course. Lattice people haven't talked about it because the signals are noisier, and because there is no chiral Lagrangian paradigm.

The double pole would reappear if the sea quarks and valence quarks had different masses. Its residue would be proportional to the difference of the sea and valence pseudoscalar squared masses. A convenient form of partial quenching is in fact to compute hadronic properties for one set of sea quark masses (because each set is expensive) and many values of valence quark masses (because each set is cheap),

(What is the internal flavor symmetry group of partially quenched QCD? The determinant of the valence quarks is not present in the functional integral. One can cancel the determinant by introducing N_v valence bosonic quarks, since the power of the determinant is negative for bosons. The flavor group becomes^{49,50} a graded group $SU(N_v + N_s|N_v)_L \otimes SU(N_v + N_s|N_v)_R$ which spontaneously breaks to $SU(N_v + N_s|N_v)$. The low energy effective Lagrangian has additional mesons, corresponding to bound states of quarks and bosonic quarks.)

Where the eta-prime comes in is in the calculation of corrections to tree-level relations^{50,51}. These are typically dominated by processes with internal Goldstone boson loops, contributing terms like

$$\int d^4k G(k, m) \simeq \left(\frac{m}{4\pi}\right)^2 \log\left(\frac{m^2}{\Lambda^2}\right) \quad (67)$$

(plus cutoff effects). The eta-prime hairpin can appear in these loops, replacing $G(k, m) \rightarrow -G(k, m)\lambda^2 G(k, m)$ and altering the chiral logarithm. Thus, in a typical observable, with a small mass expansion

$$Q(m_{PS}) = A\left(1 + B\frac{m_{PS}^2}{f_{PS}^2} \log m_{PS}^2\right) + \dots \quad (68)$$

quenched and $N_f = 3$ QCD can have different coefficients (different B 's in Eq. 68), seemingly randomly different. (Quenched f_π has no chiral logarithm while it does in full QCD, the coefficients of O_+ , the operator measured for B_K , are identical in quenched and full QCD, etc.) Even worse, one can find a different functional form. For example, the relation between pseudoscalar mass and quark mass in full QCD is

$$m_{PS}^2 = Am_q\left(1 + \frac{m_{PS}^2}{8\pi^2 f^2} \log(m^2/\Lambda^2)\right) + \dots \quad (69)$$

In quenched QCD, the analogous relation is

$$(m_{PS})^2/(m_q) = A[1 - \delta(\ln(m^2/\Lambda^2) + 1)] + \dots \quad (70)$$

28 *DeGrand*

where $\delta = \lambda^2/(8\pi^2 N_c f_\pi^2)$ is expected to be about 0.2 using the physical η' mass. This means that m_{PS}^2/m_q actually diverges in the chiral limit! Many quenched simulations actually search for these “quenched chiral logarithms,” and a few⁵² claim to have seen them.

Quenched QCD will not go away any time soon, but its days as a source of precision numbers for QCD matrix elements are clearly numbered. It will continue to be used for tests of methodology, as a proving ground for new ways of processing data, and a way to settle some controversies. There is also quite a bit of continuum phenomenology which can be altered to apply to quenched QCD and which simulations of quenched QCD can validate – or not⁵³.

One example of a controversy quenched QCD can address is the following: At Lattice 2000, S. Aoki⁵⁴ argued that the continuum limit of spectroscopy with staggered quarks and Wilson-type quarks might be different. This would represent a loss of universality, and would represent a serious problem for (at least) one kind of lattice discretization of fermion. The data he showed used unimproved Wilson fermions (which have order a lattice artifacts), unimproved staggered quarks, and clover quarks (both of which have $O(a^2)$ scaling violations). His observed disagreement may have been because of the large lattice artifacts in (at least some) of the data sets, which make extrapolations to $a \rightarrow 0$ difficult. An example of more recent data is shown in Fig. 7. This is an example of an “APE plot” which compares two dimensionless ratios (in this case $(m_{PS}/m_V)^2$ vs m_N/m_V). If scaling violations are absent, data from different lattice spacings will lie on a common curve. The data shown in Fig. 7 are not extrapolated to the continuum limit, but they do give reasonable evidence that there is not a lot of scale violation in quenched spectroscopy done with improved actions.

5. Simulations with Dynamical Fermions

Simulations which include dynamical fermions go back about fifteen years. Because they are so costly, people begin with fairly heavy sea quarks (pseudoscalar/vector meson mass ratios > 0.7), and try to go down. Volumes tend to be smaller, and lattice spacings tend to be coarser than quenched simulations. Statistics are a problem; the simulations have long autocorrelation times.

Over the years I can recall simulations with 2, 3, and 4 flavors of fermions, using staggered, Wilson, and clover quarks. The RBC collaboration is in the earliest stage of a dynamical fermion simulation of domain wall fermions⁵⁷. The first simulations with overlap fermions have just appeared: they cost easily a factor of a hundred times ones with Wilson quarks⁵⁸. The lattice conferences have had a steady diet of spectroscopy and matrix element calculations from these projects. But this year there seemed to be a pause. I think many people⁵⁹ have decided that they just cannot push the quark masses down far enough to be interesting, and have gone back to studying algorithms⁶⁰. (I expect to get a lot of unhappy mail about this sentence.)

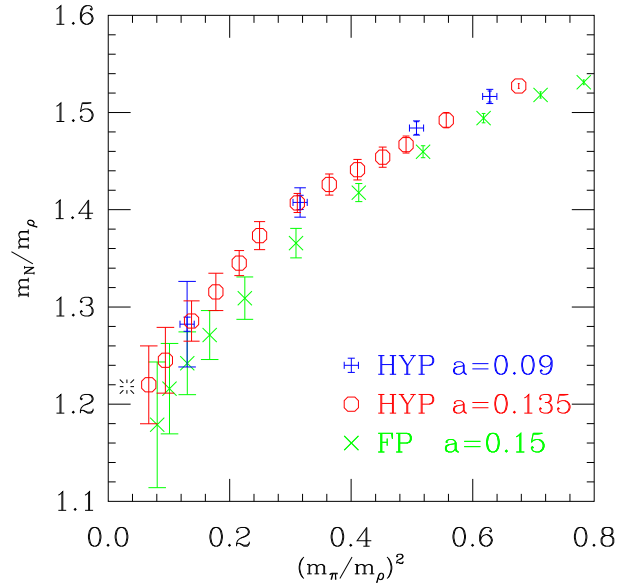


Fig. 7. A comparison of staggered spectroscopy, using an improved action, (pluses and octagons) at two lattice spacings (from Ref. 55) with that from an improved Wilson-type action (from Ref. 56) in crosses.

There is one notable exception: The most interesting lattice calculations with dynamical simulations are the ones being done by the MILC collaboration. They have combined with other groups to do calculations of spectroscopy with three flavors of dynamical staggered quarks, a strange quark at approximately its correct physical value, and degenerate up and down quarks whose masses run down to $m_s/5$. Their gauge configurations are used as backgrounds for simulations with heavy flavors. The analysis uses the taste-breaking chiral Lagrangian described in Sec. 3. They have data at two lattice spacings, 0.13 and 0.09 fm, large volumes, and high statistics. They have studied a variety of processes for which lattice methods ought to work well: spectroscopy of hadronic states which are not close to decay thresholds, properties of pseudoscalar mesons, hadrons with strange valence quarks. Their recent preprint⁶¹ presents a remarkable agreement of simulation with experiment, shown in Fig. 8.

The MILC part of the staggered project is several years old. It has produced a lot of interesting spectroscopy. One can clearly see the effects of sea quarks in the data. Here are some examples⁶².

The heavy quark potential in QCD looks something like $V(r) \simeq \sigma r - C/r$. The location of the bend in the potential is related to a quantity called the Sommer parameter r_0 (see Ref. 63) via the force, $-r^2 F(r) = 1.65$ at $r = r_0$. This corresponds to r_0 of about 0.5 fm. Fig. 9 shows the dimensionless quantity $r_0 \sqrt{\sigma}$ as a function of the quark mass, represented by $(m_\pi/m_\rho)^2$. This places the quenched approximation

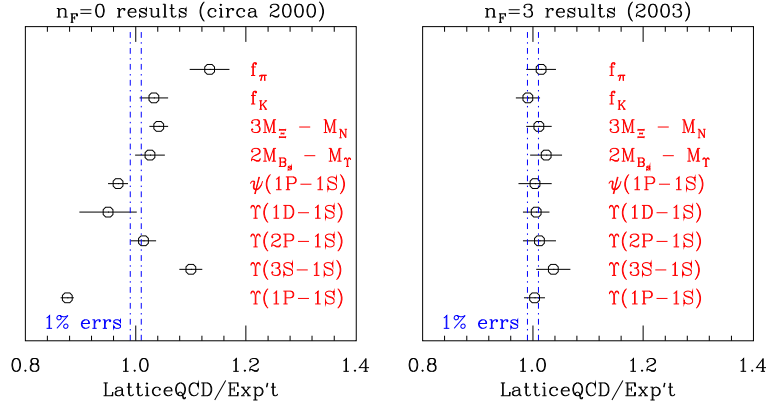
30 *DeGrand*


Fig. 8. Comparison of quenched results with results from simulations with 2+1 flavors of staggered fermions, from Ref. 61.

at $(m_\pi/m_\rho)^2 = 1$, and the chiral limit at the left side of the graph. In these plots the octagons are runs with three degenerate sea quarks, except for the rightmost point which is the quenched limit. Squares are runs with $am_s = 0.05$ at $a = 0.13$ fm. This is roughly the physical value of the strange quark mass. For these runs, $am_{u,d} < 0.05$. The isolated diamond is a two flavor run. Finally, the cross at $(m_\pi/m_\rho)^2 = 1$ is an 0.09 fm lattice spacing quenched run. From the two quenched points the authors infer that remaining lattice artifacts are small compared with the effects of the sea quarks. One can clearly see the distinction between two and three flavors, as well as the effect of using two light and one heavy flavor rather than three degenerate flavors (the “kink” at $(m_\pi/m_\rho)^2 \approx 0.46$).

Lacock and Michael⁶⁴ have observed differences between the quenched meson spectrum and the real world. They studied the quantity

$$J = m_{K^*} \frac{\partial m_V}{\partial m_{PS}^2} \quad , \quad (71)$$

where m_V and m_{PS} are the vector and pseudoscalar meson masses. This quantity has the advantage of being relatively insensitive to the quark masses, so that accurate tuning of the strange quark mass or extrapolation of the masses to the chiral limit is not essential.

Of course, to compare to experiment the derivative in this expression must be replaced by a ratio of mass differences, and MILC choose

$$J = m_{K^*} \frac{\{m_\phi - m_\rho\}}{2\{m_K^2 - m_\pi^2\}} \quad . \quad (72)$$

Here m_ρ is the mass of the vector meson including two light quarks, etc. Figure 10 shows the results for J in quenched and three flavor QCD. This is plotted versus m_{K^*}/m_K , for which the real world value is 1.8. The burst is the real world value of this definition of J (0.49), and the cross is the value of J found in the quenched

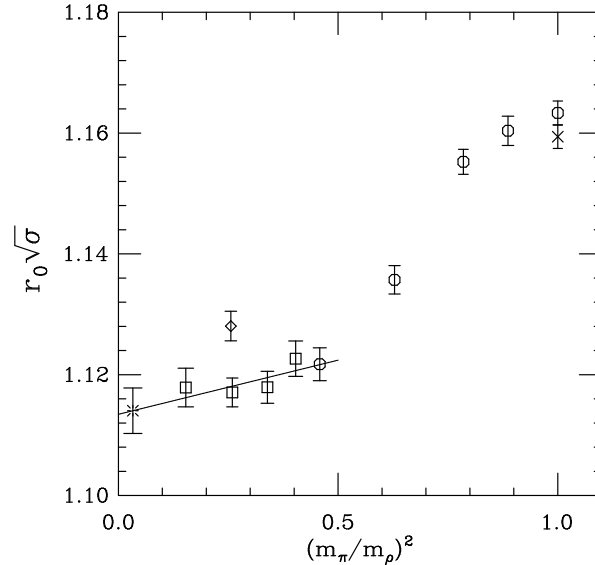


Fig. 9. Effects of dynamical quarks on the shape of the potential: $r_0\sqrt{\sigma}$ as a function of the quark mass. The two quenched points are at the far right, with the octagon coming from the 0.13 fm run and the cross from the 0.09 fm run. The remaining octagons are full QCD runs with three degenerate flavors, and the squares are full QCD runs with two light flavors and one heavy. The diamond is the two flavor run, and the burst at the left is a linear extrapolation of the 2+1 results to the physical value of $(m_\pi/m_\rho)^2$. From Ref. 62.

simulations of Ref. 64. One can see a clear effect of the sea quarks on this quantity. Figure 10 also contains one point with two dynamical flavors. This point falls near the three flavor points, indicating that the dynamical strange quark is less important than the two light quarks.

If there are dynamical fermions in the configurations, then one ought to see processes like particle decay in the simulations. What the lattice measures is energies. If a particle A could decay into a BC state, the $A - A$ correlator would have a contribution which would show an $\exp(-E_{BC}t)$ behavior, with $E_{BC} \simeq m_B + m_C$. E_A and E_{BC} might depend on simulation parameters (like quark masses) and one might look for avoided level crossings as the parameters were varied⁶⁵. (Spin models with several species of excitation show this kind of behavior⁶⁶.) The chief target is the rho meson. Evidence for a $\rho\pi\pi$ coupling has not been seen. The problem is that the rho is $J = 1$, so in the decay $\rho \rightarrow \pi\pi$ the pions are P-waves. The minimum energy of a two-pion state is then $m_\pi + \sqrt{m_\pi^2 + p_{min}^2}$, where $p_{min} = 2\pi/L$ is the smallest nonzero momentum in a box of width L . This effectively pushes the threshold for the level crossing to smaller quark mass. (For further discussion of quantum number effects for staggered fermions, see Ref. 67.)

However, the instability of an excited state has been seen in a different channel, the isotriplet scalar a_0 meson⁶². It is clearly very different in the quenched and full

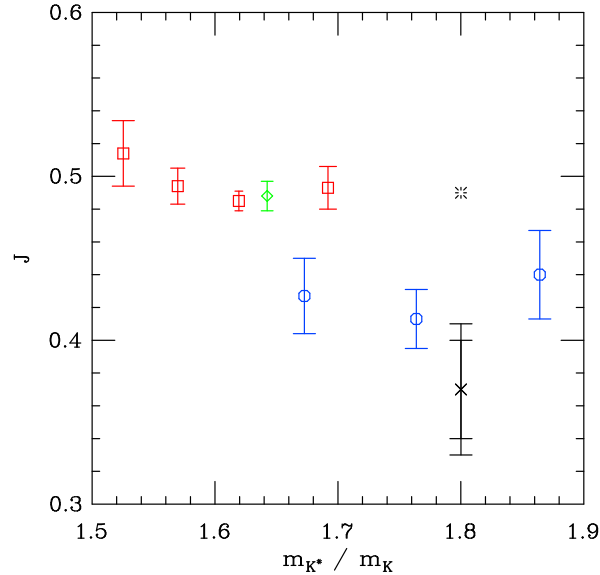


Fig. 10. The mass ratio “ J ” in the quenched and full QCD calculations. Squares are the three flavor results, and octagons are the quenched results. The diamond is the two flavor run, using a non-dynamical strange quark with mass $am_q = 0.05$. The burst is the real world value, and the cross is the quenched value of Ref. 64. The smaller error bar on the cross is the statistical error, and the larger the quoted systematic error. From Ref. 62.

QCD runs. For large quark masses there is no visible difference, but as the quark mass is decreased the full QCD 0^{++} mass drops below all the other masses. For all but the lowest quark mass, the quenched 0^{++} is close to the other P-wave meson masses. It is plausible to ascribe the behavior of the full QCD mass to the decay of the a_0 into $\pi + \eta$. (Bose symmetry plus isospin forbids decay into two pions.) Figure 11 illustrates this interpretation. In the figure I plot the quenched and full 0^{++} masses versus quark mass. The straight line in the graph is a fit to the quenched mass for the heavier quarks, and represents the mass of a $q\bar{q}$ state. The curved line with the kink at $am_q = 0.05$ represents the mass of $\pi + \eta$. For $am_q \geq 0.05$ MILC used three degenerate quark flavors, so the η and π are degenerate and this line is simply twice the pion mass. For $am_q < 0.05$ one does not have direct information on the η mass, so the Gell-Man–Okubo formula written in terms of an “unmixed $s\bar{s}$ ” mass (just the pseudoscalar mass at $am_q = 0.05$) is used:

$$m_\eta^2 = (m_\pi^2 + 2m_{s\bar{s}}^2)/3. \quad (73)$$

In the quenched case the a_0 mesons can couple to two-meson states through a “hairpin diagram” on one of the meson lines. Such diagrams can behave like powers of t times $e^{-2m_\pi t}$ and therefore masquerade as a light a_0 when $2m_\pi < m_{a_0}$. This may explain the lightest quark mass quenched point⁶⁸.

The authors of Ref. 61 argue that their results show that at last, there is a

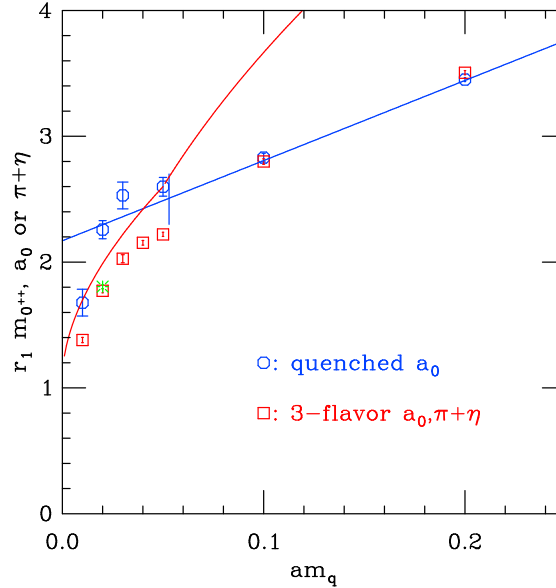


Fig. 11. 0^{++} masses versus quark mass. The lightest fitted energy in the scalar channel. Octagons are quenched results, squares are three flavor results, and the burst is the two flavor run. The straight line is a crude extrapolation of the heavy quark points. The curved line is the $\pi + \eta$ mass estimate, as discussed in the text. The short vertical line marks the approximate quark mass where the a_0 mass is twice the quenched pion mass. From Ref. 62.

workable algorithm for simulating QCD with light fermions, and that its successes mean that the time is ripe to apply it to a wide variety of lattice matrix element calculations.

However, this conclusion is not universally accepted by the lattice community. Many people are worried about the way staggered fermions are used to represent 2+1 flavors of sea quarks.

Lattice simulations treat valence quarks and sea quarks differently. Basically, valence quarks (the ones attached to the external sources) do not have any quantum numbers (other than their mass and spin). One computes classes of Feynman diagrams on the lattice, then re-weights them with global symmetry indices and bundles them together. (For example, the same propagators are used for the quark and the antiquark in a mass-degenerate meson). In staggered fermions, one uses a single flavor of staggered fermions, with its four tastes, and computes correlation functions in which the sources project (nearly) onto the same initial and final taste. The quark could hop temporarily into a different taste state as it propagates across the lattice (this would happen by emitting and absorbing hard gluons), but this is just cutoff scale physics which contributes $O(a^2 g^2)$ scale violations.

But sea quarks are different – the number of flavors matters. In the absence of flavor symmetry breaking, mass-degenerate fermions have identical spectra and one

34 *DeGrand*

can simulate N_f flavors of degenerate fermions simply by raising $\det M$ for a single flavor to the N_f power. But each taste of staggered fermions contributes to the functional integral like a single flavor of continuum quark. $\text{Det } M$ is the weighting for four continuum flavors. To get the weighting for a single flavor, people doing simulations with staggered fermions re-weight the determinant to $\det^{1/4} M$ per staggered flavor.

Are simulations with staggered fermions with $\det^{1/4} M$ fundamentally correct? Until recently, all the theory of the fractional determinant was a single sentence in a 1981 paper by Marinari, Parisi, and Rebbi⁶⁹: “On the lattice, this action ($S_G - (1/4)\text{Tr} \ln M$) will produce a violation of fundamental axioms, but we expect the violation to disappear in the continuum limit and then recover the theory with a simple fermion.” In the past year, the situation has heated up, although the literature is still sparse⁷⁰, probably because there are no well-defined questions.

It is a peculiar exchange-of-limits question. Any N -flavor action with flavor symmetry can be reduced to a one-flavor action by taking the $1/N$ th root. But in staggered fermions taste symmetry is broken by gluon interactions at nonzero lattice spacing. What does taking the fractional root before restoring flavor symmetry do?

Here is my own condensation of arguments I have participated in⁷¹:

The most serious problem could be a loss of locality. Is there a single-flavor (undoubled) local fermion action whose determinant is equal to $\det^{1/4} M$ (or equal to it up to cutoff effects)? If such an action exists, then there are no problems in principle with $\det^{1/4} M$ staggered fermions. This would certainly be something novel! Its chiral symmetry properties would certainly be very different from those of ordinary staggered fermions. Its chiral charge could not be discrete, because that would violate the Nielsen-Ninomiya theorem. There is no reason that the action could not be ultra-local, but it seems hard to combine an ultra-local action with an unquantized chiral charge. It’s easier for me to imagine that it would have couplings falling exponentially with distance. If such an action does not exist, then universality is lost. It would not be possible to integrate out short distance physics to leave a long distance effective action whose couplings flow to a fixed point, because remnants of the original action will be left behind after each blocking step.

And of course, there are many ways to define matrices whose determinants are equal. Recall the discussion at the end of the last section about taste constraints. $\text{Det } M$ was converted into $\det(M^\dagger M)^{1/2}$ by deleting fields on half the sites of the lattice. That gives a “square root” action which is ultra-local, as opposed to working with an action $(M^\dagger M)^{1/2}$, which probably isn’t local⁷⁰!

In the momentum-space decomposition of tastes (Eq. 48), each taste occupies a segment of the Brillouin zone equivalent to $-\pi/2 < p_\mu < \pi/2$ with a free field ($i\gamma_\mu \sin(p_\mu)$) dispersion relation. The Fourier transform of its inverse propagator is an action with long range (power law falloff) couplings. In the hypercube decomposition, each taste’s action (the first term of Eq. 51) is ultra-local, but tastes still mix for any finite value of a through the second term of Eq. 51.

It is certainly the case that an action with $\det^{1/4} M$ fermions is not unitarity, in the sense that absorptive parts of processes are not related to cross sections. This is a generic feature of any partially-quenched theory, where the actions of valence and sea quarks are different. Different actions mean different Feynman rules. (Even though there may be no action corresponding to $\det^{1/4} M$ fermions, one can expand $(1/4)\text{Tr} \ln M$ in a power series in g and construct graphs.) Unitarity relates processes in which quarks are internal lines (with internal vertices, propagators, etc.) to other processes where the same quarks appear as external lines. Then they would be valence quarks, with valence Feynman rules. For staggered fermions, the differences occur in processes where taste is changed. There are 4 identical vertices (per staggered flavor) which do not change taste in the determinant, but only one process which changes taste i to another taste j ($i, j = 1 \dots 4$). But taste changing interactions involve hard gluons, with momentum transfer $q_\mu \simeq \pi/a$, so maybe we are just talking about cutoff effects, again. It is also unknown whether there are practical consequences for Euclidean-space lattice calculations of non-unitarity: unitarity describes what happens when scattering amplitudes are rotated from Euclidean space to Minkowski space.

It is generally believed that “partially quenched” QCD is well-enough behaved to make predictions. Indeed there is an extensive literature⁷² on the use of partially quenched chiral perturbation theory to measure the parameters of full QCD. If the $\det^{1/4} M$ theory is local, then it is just some funny kind of partially quenched QCD⁷³ and again nothing would be wrong in principle.

There are several directions this controversy could play out:

First, someone could show analytically that there is some local action which has the same determinant as $\det^{1/4} M$, or prove that no such action exists. If such an action exists, then there is nothing wrong in principle with $\det^{1/4} M$ weighting. It would be an engineering question to ask whether this formalism is good enough to produce reliable continuum numbers. If no action exists, then QCD with $\det^{1/4} M$ weighting is not in the same universality class as continuum QCD. It would still be the case that its predictions are quite close to experiment (I am not disputing the results of Ref. 61) for many quantities, but one might be able to identify processes where it would fail. It would be like the quenched approximation all over again, only better: fundamentally uncontrolled, phenomenologically successful. I suppose an intermediate possibility is that for sufficiently smooth background configurations, $\det^{1/4} M$ could correspond to a local action, but for rough fields it might not. This is easy to visualize when one thinks of the fractional power as basically counting the geometric mean of the different taste eigenmodes: $(\prod_i^N \lambda_j)^{1/N}$. At sufficiently rough coupling, where the chiral symmetry is only a $U(1)$, the eigenmodes are no longer even approximately degenerate, and the geometric mean would not have much meaning.

Second, one could continue to compute known quantities, see that the simulations continued to agree with experiment, and go on to do make yet more predic-

tions. This is how comparison of theory and experiment generally happens. The dangerous possibility here is that something might not agree with experiment, and it might be a matrix element from a Standard Model test. Then, is the Standard Model wrong, or is it the simulation with a fractional power?

Checks with simpler models would be very useful. The Schwinger model (for different flavor number) is a good test case, and it is simple enough that it can be overwhelmed by numerical simulations. Recently, Dürr and Hoelbling⁷⁴ have begun a study of the Schwinger model, comparing overlap and staggered fermions. They have so far looked at only one lattice spacing, and so far only looked at condensate- and topological charge-related quantities. Results from overlap and staggered fermions are quantitatively different. However, agreement between staggered and overlap simulations is considerably improved by smearing the action. This is true both for $N_f = 1$ and 2. There does not seem to be anything funny happening with the $N_f = 1$ fractional root. It may just be that the differences between staggered and overlap fermions are cutoff effects, nothing more. The authors caution that their gauge configurations are much smoother than (my reading) typical $a = 0.13$ fm four-dimensional $N_f = 2 + 1$ Asqtad $SU(3)$ configurations, so one should be cautious with interpretations. More work needs to be done (and they will do it), varying the lattice spacing and checking scaling.

All dynamical fermion simulations are costly – at least a factor of 100 more than a quenched calculation done at similar values of lattice spacing and quark mass. And yet, looking back at Fig. 8, the change in the numbers which come out of the analyses, going from quenched to $2 + 1$ flavor QCD, is only a few percent. True, these are quantities which are selected to be insensitive to hadronic decay, or indeed any strong non quenching effects, but it still seems absurd – to work so hard for so little effect. In any classroom physics lecture, this discussion would be an introduction to a description of how to do a perturbative calculation, systematically improving one’s approximate result. But no such story exists for simulations of QCD⁷⁵.

6. Hadronic Matrix Elements from the Lattice

One of the major goals of lattice calculations is to provide hadronic matrix elements which either test QCD or can be used to provide low energy hadronic matrix elements as inputs to test the standard model. A wide variety of matrix elements can be computed on the lattice (compare Fig. 12) and used to extract CKM mixing angles from experimental data. A new organization, the Lattice Data Group, <http://www.cpt.univ-mrs.fr/ldg/>, is attempting to build a “lattice wallet card” of relevant results.

The lattice enters at a rather late stage of the calculation. Consider some “generic” electroweak process. Viewed at the shortest distance scale, a distance $\Delta x \simeq 1/M_W$, quarks emit and absorb W and Z bosons. However, physical hadrons containing u , d , s , c , or b quarks are big objects, a fraction of a fermi in size, and they

cannot “see” the highly virtual W and Z bosons. Their interactions are described by a low-energy effective field theory valid at scales μ of a few GeV, which would be constructed by integrating out short distance physics using the operator product expansion, combined with the renormalization group. The effective Hamiltonian basically reduces to a sum of four-fermion interactions⁷⁶. For example, single-W exchange processes would be described by

$$H_W^{eff} = \frac{G_F}{\sqrt{2}} \sum_{i=0}^{10} c_i(\mu) O_i(\mu) \quad (75)$$

where the O_i 's are four fermion operators and the c_i 's are (known) Wilson coefficients. Similarly, the (second-order weak) process $\bar{B} - B$ mixing is parameterized by the ratio $x_d = (\Delta M)_{b\bar{d}}/\Gamma_{b\bar{d}}$

$$x_d = \tau_{b\bar{d}} \frac{G_F^2}{6\pi^2} \eta_{QCD} F\left(\frac{m_i^2}{m_W^2}\right) |V_{tb}^* V_{td}|^2 b(\mu) \left\{ \frac{3}{8} \langle \bar{B} | \bar{b} \gamma_\rho (1 - \gamma_5) d \bar{b} \gamma_\rho (1 - \gamma_5) d | B \rangle \right\} \quad (76)$$

This is a typical formula used to relate an experimental number to a Standard Model prediction. It has a product of factors from phase space integrals or perturbative QCD calculations, a combination of CKM matrix elements (whose determination is presumably the primary goal), followed by a four quark hadronic matrix element. In order to extract the CKM matrix element from the measurement of x_d (and its strange partner x_s), we need to know the value of the object in the curly brackets, defined as $3/8 M_{bd}$ and parameterized as $m_B^2 f_{B_d}^2 B_{bd}$ where B_{bd} is the so-called B-parameter, and f_B is the B-meson decay constant, $\langle 0 | \bar{b} \gamma_0 \gamma_5 d | B \rangle = f_B m_B$. Lattice calculations are the most model-independent way to compute the decay constants, B-parameters, and their ratio $\xi = (f_{B_s} \sqrt{\hat{B}_{B_s}})/(f_B \sqrt{\hat{B}_B})$. (Hats denote the renormalization group invariant quantities.) The B-parameters and decay constants are scale and prescription-dependent quantities and the lattice-regulated quantities have to be converted into some continuum regularization scheme to complete the calculation.

The lattice calculation of one of these quantities involves many ingredients. First, one has to extract the lattice-regulated matrix element. Most of the matrix elements measured on the lattice are extracted from expectation values of local

$$\left(\begin{array}{ccc} \mathbf{V}_{ud} = 1 - \frac{\lambda^2}{2} & \mathbf{V}_{us} = \lambda & \mathbf{V}_{ub} = A\lambda^3(\rho - i\eta) \\ \pi \rightarrow l\nu & K \rightarrow \pi l\nu & B \rightarrow \pi l\nu \\ \mathbf{V}_{cd} = -\lambda & \mathbf{V}_{cs} = 1 - \frac{\lambda^2}{2} & \mathbf{V}_{cb} = A\lambda^2 \\ D \rightarrow l\nu & D_s \rightarrow l\nu & B \rightarrow D l\nu \\ D \rightarrow \pi l\nu & D \rightarrow K l\nu & \\ \mathbf{V}_{td} = A\lambda^3(1 - \rho - i\eta) & \mathbf{V}_{ts} = -A\lambda^2 & \mathbf{V}_{tb} = 1 \\ \langle B_d | \bar{B}_d \rangle & \langle B_s | \bar{B}_s \rangle & \end{array} \right) \quad (74)$$

Fig. 12. Matrix elements which can be computed reasonably reliably with lattice methods, and their impact on the CKM matrix. From Ref. 61.

38 *DeGrand*

operators $J(x)$ composed of quark and gluon fields. For example, if one wanted $\langle 0|J(x)|h\rangle$ one could look at the two-point function

$$C_{JO}(t) = \sum_x \langle 0|J(x,t)O(0,0)|0\rangle. \quad (77)$$

Inserting a complete set of correctly normalized momentum eigenstates

$$1 = \frac{1}{L^3} \sum_{A,\vec{p}} \frac{|A,\vec{p}\rangle\langle A,\vec{p}|}{2E_A(p)} \quad (78)$$

and using translational invariance and going to large t gives

$$C_{JO}(t) = e^{-m_A t} \frac{\langle 0|J|A\rangle\langle A|O|0\rangle}{2m_A}. \quad (79)$$

A second calculation of

$$C_{OO}(t) = \sum_x \langle 0|O(x,t)O(0,0)|0\rangle \rightarrow e^{-m_A t} \frac{|\langle 0|O|A\rangle|^2}{2m_A} \quad (80)$$

is needed to extract $\langle 0|J|A\rangle$, fitting the two correlators with three parameters.

Similarly, a matrix element $\langle h|J|h'\rangle$ can be gotten from

$$C_{AB}(t,t') = \sum_x \langle 0|O_A(t)J(x,t')O_B(0)|0\rangle. \quad (81)$$

by stretching the source and sink operators O_A and O_B far apart on the lattice, letting the lattice project out the lightest states, and then measuring and dividing out $\langle 0|O_A|h\rangle$ and $\langle 0|O_B|h\rangle$.

These lattice matrix elements are not yet the continuum matrix elements. Typically, one is interested in some matrix element defined with a particular regularization scheme. It is a generic feature of quantum field theory that an operator defined in one scheme (\overline{MS}) will be a superposition of operators in another scheme (lattice). In principle, the superposition could be all possible operators. So an operator of dimension D will mix like

$$\langle f|O_n^{cont}(\mu)|i\rangle_{\overline{MS}} = a^D \sum_m Z_{nm} \langle f|O^{latt}(a)_m|i\rangle. \quad (82)$$

The only restrictions on mixing are the ones imposed by symmetries, and generally, lattice actions have fewer symmetries than in the continuum, so operator mixing is more severe. The most serious source of mixing for light quark operators is the way lattice fermions treat chiral symmetry. Wilson-type fermions break chiral symmetry (even massless ones do so off-shell) and so nothing prevents mixing into “wrong chirality” operators. The mixing structure of overlap fermions (and domain wall fermions in the limit of infinite fifth dimension length) is basically identical to the continuum, and these formulations really come into their own in cases where chiral symmetry is important.

In Eq. 82 the mixing coefficients to lattice operators with the same dimensionality as the continuum ones term will contain the anomalous dimension matrix of the continuum operators

$$Z_{mn} = 1 + \frac{g^2}{16\pi^2}(\gamma_{mn} \log a\mu + A_{mn}) + \dots \quad (83)$$

This must happen to cancel the mu-dependence of the coefficient function, since $c(\mu)\langle f|O^{cont}|i\rangle_\mu$ is independent of the renormalization point. In principle the leading log could be summed, but in practice people don't know how much of the constant term A should be absorbed into a change of scale of g . This would involve a two loop calculation. (Brave groups⁷⁷ are beginning such calculations.) So they are just left there as constants. There are also terms for mixing with higher dimensional operators, which give contributions proportional to positive powers of a . (These are usually benign, they look just like scaling violations.) One can also have mixing with lower dimensional operators, with contributions involving negative powers of a . When they appear, these are dangerous. They must drop out in the continuum but it is a delicate business, since they look like they are growing as an inverse power of a .

People compute the Z_{nm} 's in a number of ways. Most straightforward is to use perturbation theory. For lattice actions involving thin links, lattice perturbation theory in terms of the bare coupling $g(a)$ is not very convergent: the A_{nm} 's can be very large (order 30, sometimes), so $\alpha_s A/(4\pi) \simeq 0.2$ or more. The source of this behavior is the ‘‘tadpole graph,’’ usually as part of the fermion self-energy. (See Fig. 13.) The lattice fermion-gauge field interaction looks like $\bar{\psi}(x)U_\mu(x)\psi(x+\hat{\mu})$ and $U \simeq 1 + ig_a A_\mu - g^2 a^2/2A_\mu^2 + \dots$. The $\bar{\psi}A_\mu^2\psi$ vertex, not present in any sensible continuum regularization, causes problems when the gluon forms a loop: the quadratic divergence from the loop integral combines with the a^2 to give a finite contribution—in fact, it is often the dominant contribution. In perturbation theory one must also choose the momentum scale in the running coupling constant. There are reasonable choices for how to do that^{78,79}. Perturbation theory for fat link actions is generally better behaved. The fat link vertex acts as a form factor to suppress the tadpole. Situations where $|Z| - 1$ equals 0.05 or less are not unusual⁸⁰.

Often one can find Z_{nm} 's by computing lattice Ward identities⁸¹. For example, with overlap fermions, chiral symmetry ‘‘protects’’ the combination $m_q \bar{\psi}\psi$ and constrains the (local) pseudoscalar and scalar currents, and vector and axial vector currents, to have equal renormalization constants. The matrix element of the pseudoscalar current gives $\langle 0|\bar{\psi}\gamma_5\psi|PS\rangle = f_{PS}^P m_{PS}^2/(2m_q)$, with no lattice-to-continuum renormalization factor for f_{PS}^P ; $f_{PS}^P = f_{PS}$. The zeroth component of the axial current has as its matrix element $\langle 0|\bar{\psi}\gamma_0\gamma_5\psi|PS\rangle = f_{PS}^A m_{PS}$, with $Z_A f_{PS}^A = f_{PS}$. Thus $Z_A = f_{PS}^P/f_{PS}^A$ which can be computed by fitting a correlator with a pseudoscalar sink and a correlator with an axial vector sink, and taking the ratio. (To experts, this is slightly wrong: $m_q \bar{\psi}(1+aD)\psi$ and the point split currents $\bar{\Gamma}(1+aD)\psi$ are the quantities related by overlap current algebra. Experts

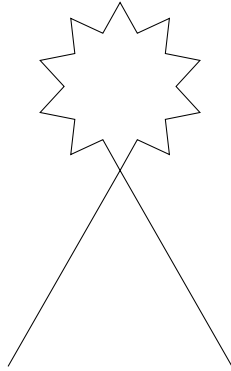


Fig. 13. The “tadpole graph” for the fermion self energy..

also know that the “ aD ” terms are removed by a slight redefinition of the lattice propagator...)

The most commonly used nonperturbative method for computing matching factors is called the “Regularization Independent” or RI scheme⁸². One computes quark and gluon Green’s functions in a smooth gauge, regulated by giving all external lines a large Euclidean squared momentum p^2 . For example, for a bilinear, one might compute an un-amputated correlation function $G_O(p,a)$. One would also compute the quark propagator in momentum space, $S(p,a)$. Then the vertex would be found by snipping the propagators off the correlator, $\Lambda_O(p,a) = S^{-1}(p,a)G_O(p,a)S^{-1}(p,a)$ and the vertex would be computed by projection: $\Gamma_O(p,a) \propto \text{Tr}\Lambda_O P_O$. Roughly speaking, the Z factor is the ratio of $\Gamma_O(p,a)$ to its free-field value, or one would match to a perturbative calculation of the vertex, regulated identically. To measure a Z -factor, one should see a plateau in the observable versus p^2 . One must stay away from large pa (where discretization effects enter) and small p (where nonperturbative physics turns on), The author has not tried doing this himself, but there are many claims in the literature from people who have, that it is straightforward to do.

People become very dogmatic about how to compute matching factors. It is a very interesting exercise to compare the points of view of a firm advocate of lattice perturbation theory⁷⁷ with that of an equally firm advocate of nonperturbative renormalization⁸³. Read these papers back to back!

6.1. *Charm and bottom matrix elements*

We spent a long section on relativistic fermions, so the reader will not be surprised to learn that there are also many choices for discretizing heavy fermions. It is very difficult⁸⁴ to do direct calculations with relativistic b quarks because the lattice spacing is much greater than the b quark’s Compton wavelength (or the UV cutoff is below m_b). However, it might be better to think of the lattice theory as an effective field theory for low-momentum physics in the presence of two high energy scales—the

cutoff (inverse lattice spacing) and the heavy quark mass. The effects of the short distance are lumped into coefficients of the effective theory⁸⁵. A simple example of such a theory would be the standard clover action, since it has lattice versions of every operator with dimension ≤ 5 . So the simulation involves a heavy clover quark and (perhaps) some other type of light quark. The heavy quark dispersion relation is $E(p) \simeq m_1 + p^2/(2m_2) + \dots$ (if $p \ll m$) and it might happen that $m_1 \neq m_2$ because of discretization artifacts. The heavy quark magnetic moment is $\mu = 1/m_3$ and again, $m_3 \neq m_2 \neq m_1$. But m_1 is just an overall constant, so one could shift the measured hadron mass by $m_2 - m_1$ and tune the shifted mass to the desired value (to do the simulation at the physical B mass, for example). The lattice magnetic moment could also be tuned (by varying the coefficient of the clover term) using (say) the $B^* - B$ hyperfine splitting. Hadronic parameters not used to determine the lattice parameters are then objects of calculation.

Nonrelativistic QCD has also been discretized and used to make very precise calculations of the properties of quarkonia⁸⁶. This formalism can also be used for the heavy quark in a B or D meson (again as long as its momentum is small.) The “static” limit (infinite b -quark mass) is often used as an additional point on the curve. Then one can try to interpolate all the way from light quarks to heavies and get all the decay constants at once.

Another new development is the use of staggered quarks for the light quark in a heavy-light system⁸⁷. This will allow one to get to smaller quark masses than Wilson-type valence quarks permit, which will be important for chiral extrapolations. Overlap light quarks are even prettier⁸⁸ but much more costly. Calculations using overlap fermions will probably appear next year.

Early form of fat links failed rather spectacularly^{89,90} when used with heavy flavor simulations because they smeared away the short distance part of gluonic interactions, but HYP links have been used to enhance the signal of static-light correlators⁹¹.

An important systematic effect is the use of unphysical (too heavy) values of the light quark masses both in quenched and unquenched simulations. People had just been doing linear extrapolations to get down to the physical light quark mass, but this is not correct^{92,93,94}! One has to use chiral perturbation theory, with its non-analytic (logarithmic) behavior at small m_q . An example of such behavior is

$$\begin{aligned} \frac{f_{B_s}}{f_B} - 1 &= (m_K^2 - m_\pi^2) f_2(\Lambda) \\ &- \frac{1 + 3g^2}{(4\pi f_\pi)^2} \left[\frac{1}{2} I(m_K) + \frac{1}{4} I(m_\eta) - \frac{3}{4} I(m_\pi) \right] \end{aligned} \quad (84)$$

where $I_P(m_{PS}) = m_{PS}^2 \ln(m_{PS}^2/\Lambda^2)$ and f_2 is a low-energy constant. Kronfeld and Ryan⁹² pointed out that the inclusion of chiral logarithms in the chiral extrapolation of lattice data for heavy-light decay constants can drastically change f_{B_s}/f_B and ξ . By assuming $g^2 = g_{D^*D\pi}^2 = 0.35$ ⁹⁵ and $f_2 = 0.5(3) \text{ GeV}^{-2}$, they concluded that $\xi = 1.32 \pm 0.10$, which is more than 10 per cent larger than Ryan’s 2001 global

42 *DeGrand*

lattice estimate⁹⁶.

Most lattice results are done in quenched approximation. In many cases, all the other systematics (extrapolation to the continuum, matching factors, etc.) can be beaten down to below a few per cent. But the quenching systematic won't go away until dynamical fermion simulations are done.

There are many lattice calculations of f_B , f_D , B_B , and form factors for semileptonic decay. My summary leans rather heavily on reviews by Wittig⁹⁷, Becirevic⁹⁸, and Kronfeld⁹⁹.

The decay constant is computed by combining a heavy quark and a light anti-quark propagator into Eq. 77. Decay constants probe very simple properties of the wave function: in the nonrelativistic quark model $f_M = \psi(0)/\sqrt{m_M}$, where $\psi(0)$ is the $\bar{q}q$ wave function at the origin. For a heavy quark (Q) light quark (q) system $\psi(0)$ should become independent of the heavy quark's mass as the Q mass goes to infinity, and in that limit one can show in QCD that $\sqrt{m_M}f_M$ approaches a constant.

The lattice calculation of decay constants which I know best is by the MILC collaboration, again, Refs. 90 ($N_f = 2$) and 100 ($N_f = 2 + 1$, preliminary results). These authors have done careful simulations, in quenched, 2-flavor, and 2+1 flavor QCD, at many values of the lattice spacing, which allows one to extrapolate to the continuum limit by brute force. Examples of results are shown in Figs. 14 and 15. The first figure shows $f\sqrt{M}$ vs $1/M$, with data extending from the static limit to below the D . One would fit this data to a power series in $1/M$ to get to the B or D . Notice that the simple heavy quark assumption $f_M \propto 1/\sqrt{M}$ fails by 50 per cent at the B .

A plot of the data which goes into Fig. 14 is shown in Fig. 15. There does not seem to be a lot of lattice spacing dependence. Quenched data extends to smaller lattice spacing, and so one might want to use its slope to extrapolate to the continuum. The two $a = 0$ points show different extrapolation choices, clearly a source of uncertainty.

Figure 16 from Ref. 100 shows how f_B changes as the sea quarks switch on – a jump from 170 to 210 MeV. The ratio f_{B_s}/f_B , shown in Fig. 17, seems to be much more stable. Sometimes, apparently, quenching works well, sometimes not.

Semileptonic decays involve evaluating lattice correlators of three-point functions (two mesons and the current). One just fits the data (measured hopefully at many masses and as many momenta as possible—remember, momentum is quantized to be a multiple of $2\pi/L$ in a box of size L) to the expected set of form factors. For example, in $B \rightarrow \pi\ell\nu$,

$$\langle \pi(p) | V_\mu | B(p') \rangle = f^+(q^2) [p' + p - \frac{m_B^2 - m_\pi^2}{q^2} q]_\mu + f^0(q^2) \frac{m_B^2 - m_\pi^2}{q^2} q_\mu. \quad (85)$$

The best signals come when the momenta of the initial and final hadron are small. Then the large B mass forces q^2 ($q =$ lepton 4-momentum $= p_B - p_\pi$) to be large. If the form factor is needed at $q^2 \sim 0$, a large extrapolation is needed, and there will

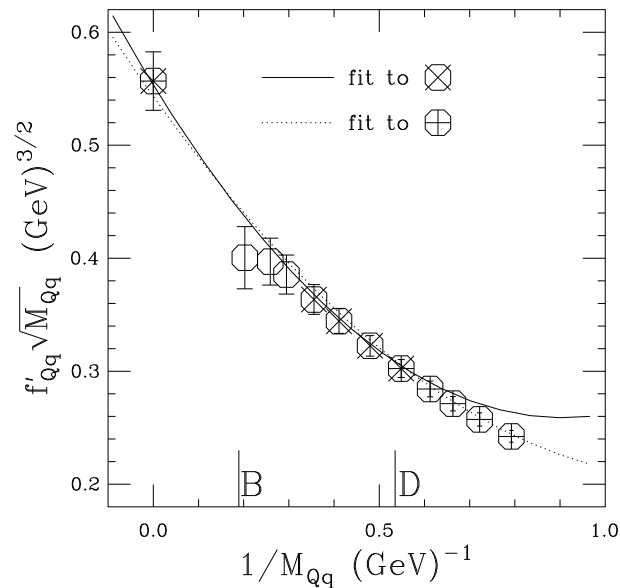


Fig. 14. Pseudoscalar meson decay constant vs $1/M$, from Ref. 90.

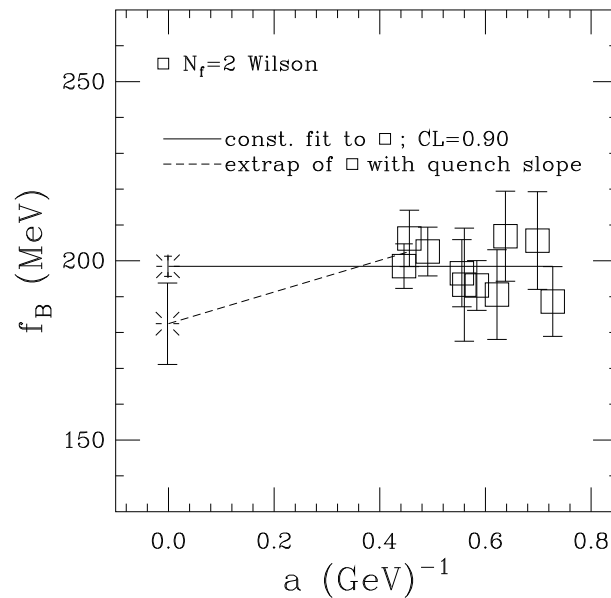


Fig. 15. f_B vs. a from Ref. 90, showing extrapolations to the continuum limit of full QCD data.

be additional errors and model dependence in the answer. (Lattice people have no advantage over anyone else at guessing functional forms.) However, finding V_{ub} from experimental data only requires knowing the form factor at one value of q^2 . This

44 DeGrand

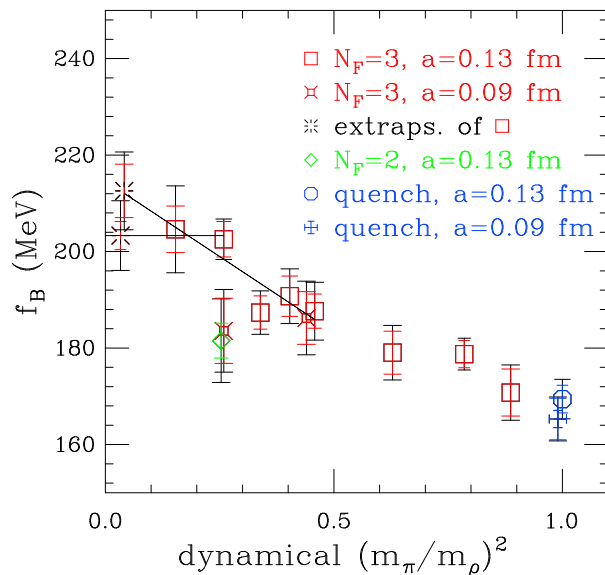


Fig. 16. f_B as a function of dynamical quark mass (plotted as $(m_\pi/m_\rho)^2$) from Ref. 100. There appears to be a considerable shift as the sea quarks drop in mass.

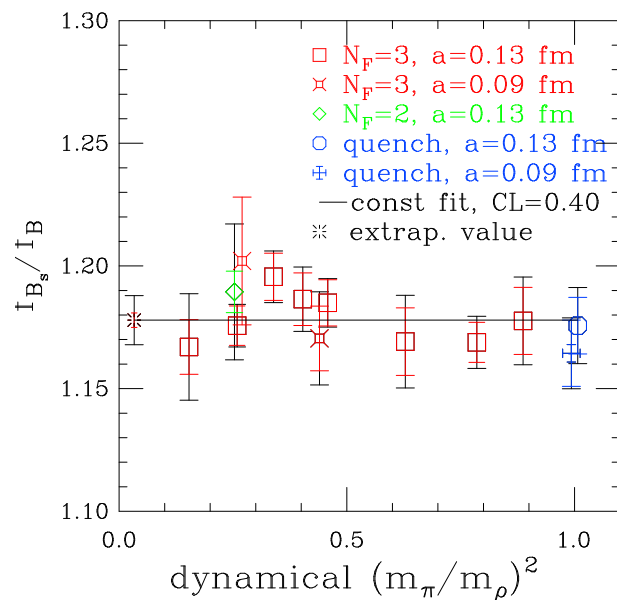


Fig. 17. f_{B_s}/f_B as a function of dynamical quark mass (plotted as $(m_\pi/m_\rho)^2$) from Ref. 100. This ratio is almost independent of the sea quark mass.

should work so long as the experiment has enough data to measure the differential rate around that region of q^2 .

As an example of a recent approach, the FNAL group has measured $B \rightarrow D\ell\nu$ and $B \rightarrow D^*\ell\nu$ form factors at zero recoil¹⁰¹. They have a clever technique for removing much of the lattice-to-continuum Z-factors by computing ratios of matrix elements. For example, in $B \rightarrow D\ell\nu$, the differential cross section at zero recoil involves a form factor $h_+(v \cdot v' = 1)$. This quantity is one in the heavy quark limit¹⁰² with corrections¹⁰³ which start at $1/m_c^2$. The lattice calculation uses lattice operators and needs to be matched to a continuum result. The FNAL group extracted it from the dimensionless ratio

$$\frac{\langle D|\bar{c}\gamma_0 b|\bar{B}\rangle\langle\bar{B}|\bar{b}\gamma_0 c|D\rangle}{\langle D|\bar{c}\gamma_0 c|D\rangle\langle\bar{B}|\bar{b}\gamma_0 b|\bar{B}\rangle} = |h_+(v \cdot v' = 1)|^2 \quad (86)$$

The denominators are just diagonal matrix elements of the charge density, (i.e. they are basically just charges) and the ratio of renormalizations between numerator and denominator is under better control than the individual factors. The $B \rightarrow D^*\ell\nu$ calculation is similar. Their calculation of its form factor is $h(1) = 0.913$ with a combined non-quenching error of about two per cent. Using this number in conjunction with experimental measurements of the branching ratio would give about a five per cent uncertainty in $|V_{cb}|$, not including the quenching uncertainty, of course.

Finally, ξ . I know of two published calculation of ξ in $N_f = 2$ QCD, which includes chiral logarithms in their analysis. The first is by the JLQCD collaboration¹⁰⁴. Their quark masses ($0.7m_s < m_q < 2.9m_s$) are too large to actually see any chiral logarithm, but they can bound the size of the effect through their inability to see it. Recently, Wingate et al¹⁰⁵ presented results (from simulations using Asqtad valence quarks on the MILC Asqtad background configurations) which are consistent with the behavior expected from chiral logarithms. A value of ξ well away from unity is suggested, about 1.25. Kronfeld's summary is shown in Fig. 18. The light quark data of Ref. 105 tracks the fit of Ref. 104. However, it happens that the decay constants of the two groups are quite different: about 260 MeV for Ref. 105 as opposed to 215 MeV for Ref. 104. Errors in both cases are claimed to be about ten per cent from all sources. Clearly something is not working... A glance at Fig. 16 shows a third prediction for f_B of about 210 MeV (from f_B , see Fig. 16), $\times 1.2$ for ξ from Fig. 17 $\simeq 250$ MeV, with maybe a ten per cent error.

6.2. Kaon Matrix Elements

6.2.1. B_K

The kaon B-parameter B_K , defined as the matrix element of a particular four fermion operator O_+ ,

$$\frac{8}{3}(m_K f_K)^2 B_K = \langle\bar{K}|\bar{s}\gamma_\mu(1 - \gamma_5)d\bar{s}\gamma_\mu(1 - \gamma_5)d|K\rangle, \quad (87)$$

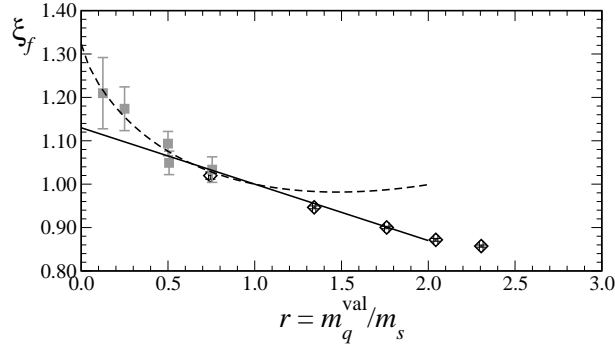


Fig. 18. ξ vs quark mass. The black points are from Ref. 104 while the grey ones are from Ref. 105. The straight line is a linear extrapolation and the dotted line is a chiral logarithm fit, both from Ref. 104. This picture is from the review of Kronfeld⁹⁹.

is an important ingredient in the testing of the unitarity of the Cabibbo-Kobayashi-Maskawa matrix¹⁰⁶. It has been a target of lattice calculations since the earliest days of numerical simulations of QCD. B_K puts a severe test on the chiral behavior of lattice simulations and so it is a useful test of methodology (in addition to being a dimensionless number interesting to experiment). There has been a continuous cycle of lattice calculations using fermions with ever better chiral properties. Unfortunately, to date all calculations (except one preliminary one described below) have been done in quenched approximation, and so there is no lattice prediction relevant to experiment.

The first lattice calculations of B_K were done with Wilson-type actions. These actions break chiral symmetry. This is a problem, because while the matrix element of O_+ scales as m_{PS}^2 , the opposite chirality operators which appear under mixing have matrix elements which are independent of m_{PS} . The signal disappears under the background in the chiral limit. Techniques for handling operator mixing have improved over the years, (for recent results, see Refs. 107-110) but I think this approach is still very difficult.

Staggered fermions (Refs. 111-112) have enough chiral symmetry at nonzero lattice spacing, that operator mixing is not a problem. One can obtain extremely precise values for lattice-regulated B_K at any fixed lattice spacing. However, to date, all calculations of B_K done with staggered fermions use “unimproved” (thin link, nearest-neighbor-only interactions), and scaling violations are seen to be large. For example, the JLQCD collaboration¹¹² saw a thirty per cent variation in B_K over their range of lattice spacings. Fat link calculations are in progress¹¹³.

For domain wall fermions, chiral symmetry remains approximate, though much improved in practice compared to Wilson-type fermions. Two groups^{114,115} have presented results for B_K with domain wall fermions. Ref. 114 has data at two lattice spacings and sees only small scaling violations. There is a few standard deviation disagreement between the published results of the two groups.

Finally, overlap actions have exact chiral symmetry at finite lattice spacing. All operator mixing is exactly as in the continuum¹¹⁶. Two groups^{117,118} have recently presented results for B_K .

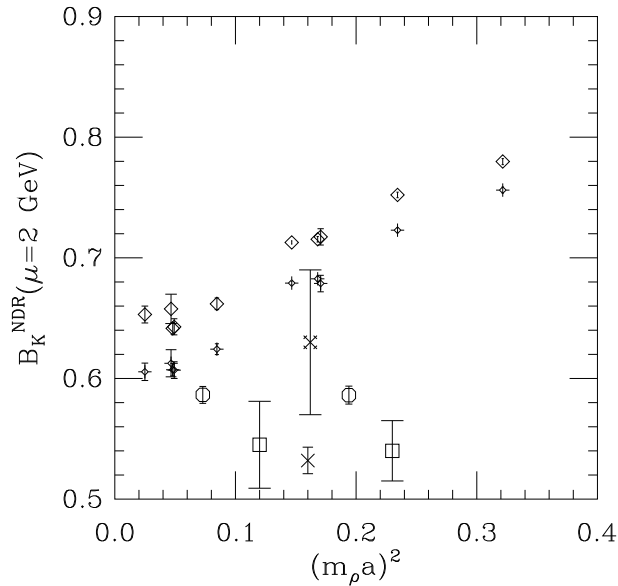


Fig. 19. B_K comparisons vs lattice spacing, from a selection of simulations with reasonably small error bars. Results are labeled diamonds and fancy diamond, Ref. 112, the fancy cross, Ref. 117, octagons, Ref. 114, the cross, Ref. 115, and squares, Ref. 118.

Figure 19 shows results for B_K at various lattice spacings, for a selection of simulations which have reasonable statistics and small error bars. Figure 20 presents results which are either extrapolated to the continuum limit, or presented by their authors as having small lattice spacing artifacts.

B_K shows quite a bit of nonlinear quark mass dependence (compare Fig. 21 for a typical recent result). This suggests strongly that chiral logarithms are present in the data, and it is reasonably easy to fit the data including their effects, out to quark masses which are about equal to the strange quark's mass. It happens that the coefficient of the chiral logarithm is the same in full and quenched QCD.

The only group reporting results for a calculation of B_K in unquenched QCD that I am aware of is the RBC collaboration, using domain wall fermions¹¹⁹. At this year's lattice conference, they presented a preliminary number of $B_K^{\text{NDR}}(\mu = 2 \text{ GeV}) = 0.50(2)$ for $N_f = 2$. It is low compared to all the quenched B_K results quoted above. This is interesting: a too-low value of B_K moves the region in the (ρ, η) plane of the CKM matrix allowed by B_K (actually, ϵ_K) away from the heavy flavor determinations. The authors do not claim anything so grand; their calculation is still in its early stages. Phenomenologists should keep an eye on their result,

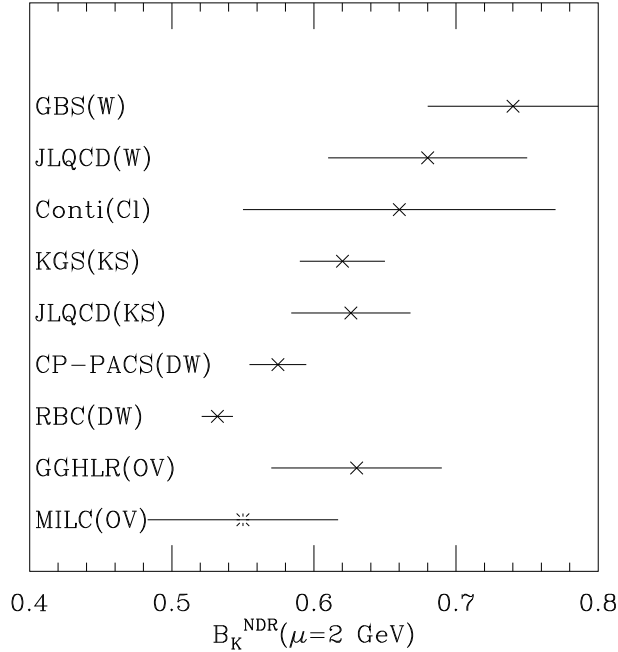


Fig. 20. B_K comparisons presented “as if” they were taken to the continuum limit. The label in parentheses characterizes the kind of lattice fermions used: W for Wilson, Cl for Clover, KS for staggered, DW for domain wall, and OV for overlap fermions. References are GBS, Ref. 107, JLQCD(W), Ref. 110, Conti, Ref. 109, KGS, Ref. 111, JLQCD(KS), Ref. 112, CP-PACS, Ref. 114, RBC, Ref. 115, GGHLR, Ref. 117, and MILC 118. The points of Refs. 110, 111, 112, 114, and 118 are the results of a continuum extrapolation; all the rest are simulations at one lattice spacing.

however.

6.2.2. $K \rightarrow \pi\pi$ and ϵ'/ϵ

There are two types of CP violating decays of kaons. The first (and largest) origin is the admixture of a small amount of a CP eigenstate into the wave function of a particle which is dominantly of the other eigenstate. This is called “indirect CP violation,” as opposed to “direct CP violation,” in which the decay of the large component of the wave function violates CP. The ratio of these two processes is parameterized by the ratio

$$\frac{\epsilon'}{\epsilon} = (16.6 \pm 1.6) \times 10^{-4} \quad (88)$$

where I am quoting its 2003 experimental value, from the review of Buras¹²¹, based on experimental data of Refs. 122, 123, 124, 125.

About two years ago, the RBC¹¹⁵ and CP-PACS¹²⁶ collaborations computed ϵ'/ϵ in quenched approximation, using domain wall fermions. Their numbers are

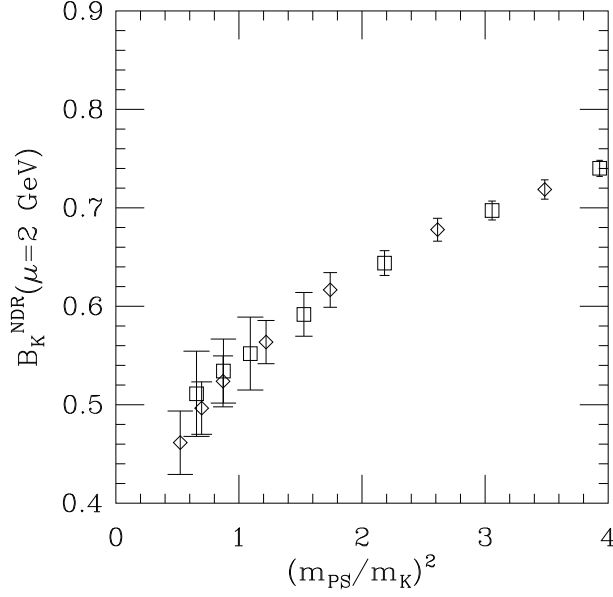


Fig. 21. A typical (not very good) lattice calculation¹¹⁸ of $B_K^{NDR}(\mu = 2 \text{ GeV})$ as a function of quark mass from the two data sets—diamonds for $a = 0.13 \text{ fm}$, squares for $a = 0.09 \text{ fm}$.

in spectacular disagreement with Eq. 88: Ref. 115 quotes $-7.7(2) \times 10^{-4}$ and Ref. 126 says that their value is “negative, and has a magnitude of order 10^{-4} . What is going on?”

Lattice calculations of ϵ'/ϵ are complicated. They begin with the low energy effective Lagrangian of Eq. 75 to compute (first) $K \rightarrow \pi\pi$ amplitudes

$$K^0 \rightarrow (\pi\pi)_I = A_I \exp(i\delta_I) \quad (89)$$

and the parameter related to the $\Delta I = 1/2$ rule,

$$\frac{1}{\omega} = \frac{\text{Re}(A_0)}{\text{Re}(A_2)} \approx 22. \quad (90)$$

These feed into the expression for ϵ'/ϵ , which happens to be dominated by the difference of two of the operators, the QCD penguin

$$Q_6 = (\bar{s}d)_L ((\bar{u}u)_R + (\bar{d}d)_R + (\bar{s}s)_R), \quad (91)$$

and the electroweak penguin

$$Q_8 = \frac{1}{2}(\bar{s}d)_L ((2\bar{u}u)_R - (\bar{d}d)_R - (\bar{s}s)_R), \quad (92)$$

$$\frac{\epsilon'}{\epsilon} \approx \frac{\omega G_F}{2|\epsilon|\text{Re}A_0} \text{Im}(V_{ts}V_{td}^*) \times \quad (93)$$

$$\left(y_6(\mu) \langle Q_6 \rangle_{I=0}^{\overline{MS}}(\mu) - \frac{1}{\omega} y_8(\mu) \langle Q_8 \rangle_{I=2}^{\overline{MS}}(\mu) \right) \quad (94)$$

50 *DeGrand*

and $\langle Q_i \rangle_I \exp(i\delta_I) = \langle \pi\pi | Q_i | K \rangle$.

People don't calculate $K \rightarrow \pi\pi$ directly on the lattice; it is difficult¹²⁷ to extract the phase shifts from the $\pi\pi$ final state interactions from lattice data (never mind trying to separate the two pions to asymptotically great distances). Instead, they use chiral perturbation theory¹²⁹ to relate $K \rightarrow \pi\pi$ amplitudes to $K \rightarrow \pi$ and $K \rightarrow$ vacuum. In the case of the $\Delta I = 3/2$ amplitude there is a factor of two change in the lattice result depending on whether tree level or one loop chiral perturbation theory is used. This is shown in an old figure from Ref. 128 in Fig. 22.

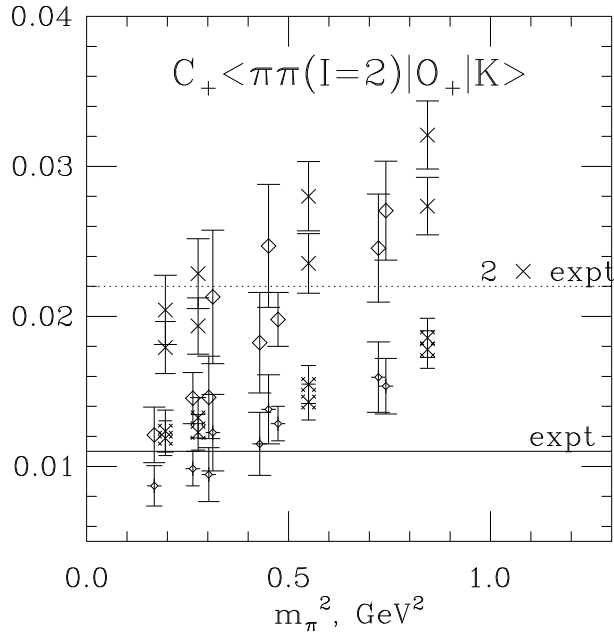


Fig. 22. $\Delta I = 3/2$ $K \rightarrow \pi\pi$ amplitude with (fancy symbols) and without (plain symbols) one-loop corrections of quenched chiral perturbation theory. Data are crosses and fancy crosses, Ref. 130; diamonds and fancy diamonds, Ref. 131.

At the end of the day, there is also a conversion from the lattice regulated matrix element to the continuum-regulated ones. This can be done either perturbatively (worrying about how convergent the calculation is) or nonperturbatively.

The quenched approximation is a real problem. Recall that the flavor symmetry of quenched QCD is not $SU(3)_L \otimes SU(3)_R$, it is the graded algebra $SU(N|N)_L \otimes SU(N|N)_R$. Consequently, the flavor content of penguin operator O_6 is altered: it came from running short distance physics down to long distance using unquenched QCD evolution, but then it is going to be evaluated in quenched approximation. Extra low energy constants appear, which would not be present in full QCD¹²⁰.

As a practical consequence, matrix elements of these operators have a chiral extrapolation similar to that of B_K ,

$$\langle \pi | O_i | K \rangle = C \left(1 + \frac{\xi m_{PS}^2}{(4\pi f)^2} \ln(m_{PS}^2) \right) + b m_{PS}^2. \quad (95)$$

Golterman and Pallente¹²⁰ computed the coefficients for chiral logarithms in quenched and partially-quenched QCD, and found that $\xi = 0$ for O_8 (in quenched approximation and in the degenerate-mass limit). This is different from in full QCD. After seeing the rather large curvature of B_K in Fig. 21, plausibly effect of a chiral logarithm, this discovery is cause for unease.

Another peculiarity of the quenched approximation is that the B-parameters for many of these operators go to zero in the chiral limit, because m_{PS}^2/m_q diverges. Recall that the B-parameters for these operators are defined as the ratio of the operator to its vacuum-saturated approximation. For left-right operators,

$$B_i^{3/2} = \frac{\langle K | O_i^{3/2} | \pi \rangle}{c_P \langle \pi | \bar{\psi} \gamma_5 \psi | 0 \rangle \langle 0 | \bar{\psi} \gamma_5 \psi | K \rangle + c_A \langle \pi | \bar{\psi} \gamma_\mu \gamma_5 \psi | 0 \rangle \langle 0 | \bar{\psi} \gamma_\mu \gamma_5 \psi | K \rangle} \quad (96)$$

where the c_i 's are numerical coefficients. The PCAC relation says that $\langle 0 | \bar{\psi} \gamma_5 \psi | PS \rangle = \frac{1}{2} m_{PS}^2 / m_q f_{PS}$. The divergence of $(m_{PS}^2/m_q)^2$ in the denominator is not compensated by any singular behavior in the numerator.

My conclusion is that we should be happy that people are building all the tools to do these calculations, and that one shouldn't take any of the quenched numbers seriously. RBC and CP-PACS are doing simulations in full QCD, and it will be interesting to see what they find when they revisit ϵ'/ϵ in the next few years. I suspect that ϵ'/ϵ will teach us more about how to do calculations than about whether the Standard Model is right or not.

7. Instead of conclusions

Lattice QCD is in a period of rapid evolution. The quenched approximation is fading out as a vehicle for precise calculations of quantities to be directly compared with experiment. It was helped on its way by algorithms for simulating QCD while preserving flavor and chiral symmetry, which cause one to attempt to do problems whose analysis forces one to confront the fundamental differences between quenched and full QCD. Simulations are beginning to reveal the presence of quenched chiral logarithms at small quark mass.

Full QCD simulations are being used in phenomenology as never before. The authors of Ref. 61 are carrying out an extensive program of light and heavy flavor physics using Asqtad dynamical fermions. They argue that essentially all the entries of the CKM matrix (except V_{tb}) can be impacted by lattice calculations whose systematics are well understood. Asqtad fermions will eliminate the unknown quenching systematic. Results from these simulations are already appearing, and more will appear within a year.

A big part of the lattice QCD computing resources in this country will go into the construction of large sets of Asqtad lattices, which the idea of making the data sets publicly available. Other people will use their configurations as “background fields” for other matrix element calculations. In many cases the cost of the simulations which are needed directly to compute a particular matrix element is much smaller than the cost of generating the configuration with its dynamical light quarks. Quenching systematics would presumably be a thing of the past. These calculations promise fantastic improvement in the quality of lattice determinations of hadronic matrix elements.

The MILC collaboration is also planning to push to smaller lattice spacing and to smaller nonstrange quark mass. Recall that their present simulations are done at $m_{u,d}/m_s \simeq 1/5$, while in the real world the ratio about $1/20$. The smallest lattice spacing in their simulations is about 0.09 fm. They estimate that the cost of this data set is about 0.8 Petaflop-hours. The cost of dropping the quark mass by a factor of two at fixed physical volume, or of dropping the lattice spacing at fixed quark mass, as given by Eq. 30, are each less than a factor of 16 increase over present simulations. They believe that a combination of these two simulations will allow extrapolations to the continuum and chiral limit at the one per cent level.

This won’t happen in a year, but it is not completely unreasonable to think about doing it. The computer resources will be there in the next decade.

However, I think that without some better understanding of the “ $\det^{1/4}$ ” replacement, all these results will be clouded by uncertainty: are these simulations fundamentally correct, or not? And I don’t think that the answer to this question will come from numerics, at least not “direct” numerics in four dimensions, like spectroscopy or matrix element calculations. I believe it is an issue of principle.

Dynamical simulations with domain wall or overlap fermions need a lot of development before they can be attempted with finite computer resources.

Lattice QCD at the end of 2004 promises to be quite different from lattice QCD at the end of 2003.

Acknowledgements

I would like to thank O. Bär, C. Bernard, C. DeTar, S. Dürr, M. Golterman, S. Gottlieb, E. Gregory, A. Hasenfratz, P. Hasenfratz, U. Heller, K. Jansen, F. Knechtli, M. Lüscher, J. Osborne, Y. Shamir, S. Sharpe, R. Sugar, D. Toussaint, G. Veneziano, and P. Weisz, for their help preparing this review, or for discussions which influenced my thinking about topics in it. I am grateful to M. Golterman Y. Shamir for a close reading of the manuscript. This work was supported by the U. S. Department of Energy.

References

1. Some standard reviews of lattice gauge theory are M. Creutz, *Quarks, Strings, and Lattices*, Cambridge, 1983, M. Creutz, ed., *Quantum Fields on the Computer*, World,

- 1992, and I. Montvay and G. Munster, *Quantum fields on a Lattice*, Cambridge, 1994. I have had recommended to me, but have not myself seen J. Smit, *Introduction to Quantum Fields on a Lattice: "a Robust Mate"*, Cambridge, 2002. The lattice community has a large annual meeting and the proceedings of those meetings (Lattice 'XX, published so far by North Holland) are the best places to find the most recent results. Other reviews which illustrate particular approaches to lattice QCD include G. P. Lepage, "Redesigning lattice QCD," hep-lat/9607076 and M. Lüscher, "Advanced lattice QCD," hep-lat/9802029. The MILC code, one of the modern packages of lattice QCD codes, is available at <http://www.physics.utah.edu/~detar/milc/>. There is even documentation.
2. K. G. Wilson, *Phys. Rev.* **D 10** 2445 (1974).
 3. Cf. H. Kluberg-Stern, A. Morel and B. Petersson, *Phys. Lett.* **B 114** 152 (1982).
 4. N. Metropolis, A. Rosenbluth, M. Rosenbluth, A. Teller, and E. Teller, *J. Chem. Phys.* **21** 1087 (1953); F. R. Brown and T. J. Woch, *Phys. Rev. Lett.* **58** 2394 (1987). M. Creutz, *Phys. Rev.* **D 36** 515 (1987).
 5. H. C. Andersen, *J. Chem. Phys.*, **72** 2384, 1980; S. Duane, *Nucl. Phys.* **B 257** 652 (1985), S. Duane and J. B. Kogut, *Phys. Rev. Lett.* **55** 2774 (1985), S. Gottlieb, W. Liu, D. Toussaint, R. L. Renken and R. L. Sugar, *Phys. Rev.* **D 35** 2531 (1987).
 6. S. Duane, A. D. Kennedy, B. J. Pendleton and D. Roweth, *Phys. Lett.* **B 195** 216 (1987).
 7. For a recent review, see M. Hasenbusch, "Full QCD algorithms towards the chiral limit," arXiv:hep-lat/0310029. Also see R. Frezzotti and K. Jansen, *Nucl. Phys.* **B 555** 395 (1999) [arXiv:hep-lat/9808011]; M. A. Clark and A. D. Kennedy, "The RHMC algorithm for 2 flavors of dynamical staggered fermions," arXiv:hep-lat/0309084.
 8. For examples, see A. Alexandru and A. Hasenfratz, *Phys. Rev.* **D 66** 094502 (2002) [arXiv:hep-lat/0207014]; A. Duncan, E. Eichten and J. Yoo, *Phys. Rev.* **D 68** 054505 (2003) [arXiv:hep-lat/0209123]; M. Luscher, *JHEP* **0305** 052 (2003) [arXiv:hep-lat/0304007].
 9. K. Symanzik, in *Recent Developments in Gauge Theories*, eds. G. 't Hooft, et al. (Plenum, New York, 1980) 313; in *Mathematical Problems in Theoretical Physics*, eds. R. Schrader et al. (Springer, New York, 1982); *Nucl. Phys.* **B 226** 187, 205 (1983).
 10. P. Weisz, *Nucl. Phys.* **B 212** 1 (1983). M. Luscher and P. Weisz, *Commun. Math. Phys.* **97** 59 (1985) [Erratum-ibid. **98** 433 (1985)].
 11. M. Luscher and P. Weisz, *Phys. Lett.* **B 158** 250 (1985).
 12. For a review, see P. Hasenfratz, "The theoretical background and properties of perfect actions," arXiv:hep-lat/9803027.
 13. C. W. Bernard *et al.* [MILC Collaboration], *Nucl. Phys. Proc. Suppl.* **73** 198 (1999) [arXiv:hep-lat/9810035].
 14. M. Albanese *et al.* [APE Collaboration], *Phys. Lett.* **B 192**, 163 (1987); M. Falcioni, M. L. Paciello, G. Parisi and B. Taglienti, *Nucl. Phys.* **B 251** 624 (1985).
 15. K. Orginos, D. Toussaint and R. L. Sugar [MILC Collaboration], *Phys. Rev.* **D 60** 054503 (1999) [hep-lat/9903032].
 16. A. Hasenfratz and F. Knechtli, *Phys. Rev.* **D 64** 034504 (2001) [arXiv:hep-lat/0103029].
 17. C. W. Bernard and T. DeGrand, *Nucl. Phys. Proc. Suppl.* **83**, 845 (2000) [arXiv:hep-lat/9909083].
 18. T. DeGrand, A. Hasenfratz and T. G. Kovacs, *Phys. Rev.* **D 67** 054501 (2003) [arXiv:hep-lat/0211006].
 19. L. H. Karsten and J. Smit, *Nucl. Phys.* **B 183**, 103 (1981).
 20. S. Adler, in *Lectures on Elementary Particles and Quantum Field Theory (1970 Bran-*

54 *DeGrand*

- deis Summer Institute in Theoretical Physics*). MIT Press, 1970.
21. H. B. Nielsen and M. Ninomiya, *Phys. Lett.* **B105** 219 (1981); *Nucl. Phys.* **B193** 173 (1981); *Nucl. Phys.* **B185** 20 (1981); See also D. Friedan, *Commun. Math. Phys.* **85**, 481 (1982).
 22. B. Sheikholeslami and R. Wohlert, *Nucl. Phys. B* **259** 572 (1985).
 23. Examples of these actions include: M. G. Alford, T. R. Klassen and G. P. Lepage, *Nucl. Phys. B* **496** 377 (1997) [arXiv:hep-lat/9611010]; T. DeGrand [MILC Collaboration], *Phys. Rev. D* **58** 094503 (1998) [arXiv:hep-lat/9802012]; C. Gattringer *et al.* [BGR Collaboration], “Quenched spectroscopy with fixed-point and chirally improved fermions,” arXiv:hep-lat/0307013.
 24. R. Frezzotti, P. A. Grassi, S. Sint and P. Weisz, *Nucl. Phys. Proc. Suppl.* **83**, 941 (2000) [arXiv:hep-lat/9909003]. R. Frezzotti, P. A. Grassi, S. Sint and P. Weisz [Alpha collaboration], *JHEP* **0108**, 058 (2001) [arXiv:hep-lat/0101001]. See also R. Frezzotti and G. C. Rossi, “Twisted-mass lattice QCD with mass non-degenerate quarks,” arXiv:hep-lat/0311008.
 25. Some recent examples include M. Della Morte, R. Frezzotti and J. Heitger [ALPHA collaboration], “A lattice approach to QCD in the chiral regime,” arXiv:hep-lat/0111048, and P. Dimopoulos, J. Heitger, C. Pena, S. Sint and A. Vladikas [ALPHA Collaboration], “B(K) from twisted mass QCD,” arXiv:hep-lat/0309134.
 26. W. J. Lee and S. R. Sharpe, *Phys. Rev. D* **60** 114503 (1999) [arXiv:hep-lat/9905023].
 27. A. Patel and S. R. Sharpe, *Nucl. Phys. B* **395** 701 (1993) [arXiv:hep-lat/9210039].
 28. S. R. Sharpe, “Phenomenology from the lattice,” arXiv:hep-ph/9412243.
 29. C. Aubin and C. Bernard, *Phys. Rev.* **68** 074011 (2003) [arXiv:hep-lat/0306026]; *Phys. Rev. D* **68** 034014 (2003) [arXiv:hep-lat/0304014]. C. Aubin *et al.* [MILC Collaboration], “Pion and kaon physics with improved staggered quarks,” arXiv:hep-lat/0309088.
 30. D. B. Kaplan, *Phys. Lett. B* **288** 342 (1992) [arXiv:hep-lat/9206013];
 31. V. Furman and Y. Shamir, *Nucl. Phys. B* **439** 54 (1995) [arXiv:hep-lat/9405004].
 32. For a recent review see P. M. Vranas, “Domain wall fermions and applications,” *Nucl. Phys. Proc. Suppl.* **94**, 177 (2001) [arXiv:hep-lat/0011066]; See also T. Blum and A. Soni, *Phys. Rev. Lett.* **79** 3595 (1997) [arXiv:hep-lat/9706023];
 33. P. H. Ginsparg and K. G. Wilson, *Phys. Rev. D* **25** 2649 (1982). My favorite introduction to this subject is the review by F. Niedermayer, *Nucl. Phys. Proc. Suppl.* **73**, 105 (1999) [arXiv:hep-lat/9810026]. A more recent review of overlap simulations is L. Giusti, *Nucl. Phys. Proc. Suppl.* **119**, 149 (2003) [arXiv:hep-lat/0211009].
 34. H. Neuberger, *Phys. Lett. B* **417**, 141 (1998) [hep-lat/9707022], *Phys. Rev. Lett.* **81** 4060 (1998) [hep-lat/9806025].
 35. P. Hasenfratz, V. Laliena and F. Niedermayer, *Phys. Lett. B* **427** 125 (1998) [arXiv:hep-lat/9801021].
 36. I am paraphrasing an argument of M. Golterman and Y. Shamir, *JHEP* **0009**, 006 (2000) [arXiv:hep-lat/0007021].
 37. M. Luscher, *Phys. Lett. B* **428** 342 (1998) [arXiv:hep-lat/9802011].
 38. S. Capitani, M. Gockeler, R. Horsley, P. E. Rakow and G. Schierholz, *Phys. Lett. B* **468** 150 (1999) [arXiv:hep-lat/9908029].
 39. I. Horvath, *Phys. Rev. D* **60**, 034510 (1999) [arXiv:hep-lat/9901014].
 40. P. Hernandez, K. Jansen and M. Luscher, *Nucl. Phys. B* **552** 363 (1999) [arXiv:hep-lat/9808010].
 41. M. Golterman and Y. Shamir, *Phys. Rev. D* **68** 074501 (2003) [arXiv:hep-lat/0306002]; “Localization in lattice QCD (with emphasis on practical implications),” arXiv:hep-lat/0309027.
 42. Cf. R. G. Edwards, U. M. Heller and R. Narayanan, *Phys. Rev. D* **59** 094510 (1999)

- [arXiv:hep-lat/9811030].
43. J. van den Eshof, A. Frommer, T. Lippert, K. Schilling and H. A. van der Vorst, *Comput. Phys. Commun.* **146** 203 (2002) [arXiv:hep-lat/0202025].
 44. J. Gasser and H. Leutwyler, *Phys. Lett. B* **188**, 477 (1987); . Leutwyler and A. Smilga, *Phys. Rev. D* **46**, 5607 (1992); H. Neuberger, *Phys. Rev. Lett.* **60**, 889 (1988); *Nucl. Phys. B* **B300**, 180 (1988).
 45. A partial set of recent calculations includes: P. H. Damgaard, M. C. Diamantini, P. Hernandez and K. Jansen, *Nucl. Phys.* **B629**, 445 (2002) [arXiv:hep-lat/0112016]; P. H. Damgaard, P. Hernandez, K. Jansen, M. Laine and L. Lellouch, *Nucl. Phys. B* **B656**, 226 (2003) [arXiv:hep-lat/0211020]; P. Hernandez and M. Laine, *JHEP* **0301**, 063 (2003) [arXiv:hep-lat/0212014]. L. Giusti, M. Luscher, P. Weisz and H. Wittig, *JHEP* **0311**, 023 (2003) [arXiv:hep-lat/0309189]; W. Bietenholz, T. Chiarappa, K. Jansen, K. I. Nagai and S. Shcheredin, “Axial correlation functions in the epsilon-regime: A numerical study with overlap fermions,” arXiv:hep-lat/0311012.
 46. R. Narayanan and H. Neuberger, *Phys. Lett. B* **302**, 62 (1993) [arXiv:hep-lat/9212019]. *Phys. Rev. Lett.* **71**, 3251 (1993) [arXiv:hep-lat/9308011]. *Nucl. Phys. B* **412**, 574 (1994) [arXiv:hep-lat/9307006]. *Nucl. Phys. B* **443**, 305 (1995) [arXiv:hep-th/9411108]; *Phys. Rev. D* **57**, 5417 (1998) [arXiv:hep-lat/9710089]; Y. Kikukawa and T. Noguchi, “Low energy effective action of domain-wall fermion and the Ginsparg-Wilson relation,” arXiv:hep-lat/9902022; A. Borici, *Nucl. Phys. Proc. Suppl.* **83**, 771 (2000) [arXiv:hep-lat/9909057].
 47. See A. Bode, U. M. Heller, R. G. Edwards and R. Narayanan, “First experiences with HMC for dynamical overlap fermions,” arXiv:hep-lat/9912043.
 48. F. Butler, H. Chen, J. Sexton, A. Vaccarino and D. Weingarten, *Nucl. Phys. B* **430** 179 (1994) [arXiv:hep-lat/9405003].
 49. A. Morel, *J. Phys. (France)* **48** 1111 (1987).
 50. C. W. Bernard and M. F. Golterman, *Phys. Rev. D* **46** 853 (1992) [hep-lat/9204007]; *Phys. Rev. D* **49**, 486 (1994) [arXiv:hep-lat/9306005].
 51. S. R. Sharpe, *Phys. Rev. D* **46** 3146 (1992) [arXiv:hep-lat/9205020].
 52. See S. J. Dong, T. Draper, I. Horvath, F. X. Lee, K. F. Liu, N. Mathur and J. B. Zhang, “Chiral logs in quenched QCD,” arXiv:hep-lat/0304005. An earlier review with references to many other groups’ results is H. Wittig, *Nucl. Phys. Proc. Suppl.* **119** 59 (2003) [arXiv:hep-lat/0210025].
 53. For an example of this kind of comparison, see P. Faccioli and T. A. DeGrand, “Evidence for instanton induced dynamics, from lattice QCD,” arXiv:hep-ph/0304219.
 54. S. Aoki, *Nucl. Phys. Proc. Suppl.* **94** 3 (2001) [arXiv:hep-lat/0011074].
 55. A. Alexandru and A. Hasenfratz, in preparation. Thanks to Prof. Hasenfratz for providing this figure.
 56. C. Gattringer, et al., Ref. 23.
 57. C. Dawson, “Dynamical domain wall fermions,” arXiv:hep-lat/0310055.
 58. Z. Fodor, S. D. Katz and K. K. Szabo, “Dynamical overlap fermions, results with hybrid Monte-Carlo algorithm,” arXiv:hep-lat/0311010.
 59. But not all. JLQCD is doing dynamical clover simulations with light quarks whose pseudoscalar/vector mass ratio is between 0.64 and 0.77, and with a strange quark close to its physical mass: T. Kaneko *et al.* [CP-PACS Collaboration], “Light hadron spectrum in three-flavor QCD with O(alpha)-improved Wilson quark action,” arXiv:hep-lat/0309137.
 60. Compare the discussion in R. Sommer *et al.* [ALPHA Collaboration], “Large cutoff effects of dynamical Wilson fermions,” arXiv:hep-lat/0309171.
 61. C. T. Davies *et al.* [HPQCD Collaboration], “High-precision lattice QCD confronts

56 *DeGrand*

- experiment,” arXiv:hep-lat/0304004.
62. C. W. Bernard *et al.*, *Phys. Rev. D* **64** 054506 (2001) [arXiv:hep-lat/0104002].
 63. See M. Guagnelli, R. Sommer and H. Wittig [ALPHA collaboration], *Nucl. Phys. B* **535** 389 (1998) [hep-lat/9806005] plus references therein.
 64. P. Lacock and C. Michael [UKQCD Collaboration], *Phys. Rev. D* **52** 5213 (1995) [arXiv:hep-lat/9506009].
 65. M. Luscher, *Nucl. Phys. B* **364** 237 (1991).
 66. C. R. Gattringer and C. B. Lang, *Nucl. Phys. B* **391** 463 (1993) [arXiv:hep-lat/9206004].
 67. C. W. Bernard *et al.*, *Phys. Rev. D* **48** 4419 (1993) [arXiv:hep-lat/9305023].
 68. A. Duncan, S. Pernice and J. Yoo, *Phys. Rev. D* **65**, 094509 (2002) [arXiv:hep-lat/0112036]. See also ⁴² and T. DeGrand, *Phys. Rev. D* **64**, 094508 (2001) [arXiv:hep-lat/0106001].
 69. E. Marinari, G. Parisi and C. Rebbi, *Nucl. Phys. B* **190** 734 (1981).
 70. K. Jansen, “pwd Actions for dynamical fermion simulations: Are we ready to go?,” arXiv:hep-lat/0311039.
 71. Participants in these discussions included O. Bär, M. Golterman, M. Lüscher, A. Hasenfratz, P. Hasenfratz, K. Jansen, F. Knechtli, P. Weisz, and members of the MILC collaboration: C. Bernard, S. Gottlieb, E. Gregory, U. Heller, J. Osborne, R. Sugar, D. Toussaint,
 72. S. R. Sharpe and N. Shoreh, *Phys. Rev. D* **62** 094503 (2000) [arXiv:hep-lat/0006017]. Compare, however: C. J. Lin, G. Martinelli, E. Pallante, C. T. Sachrajda and G. Villadoro, *Phys. Lett. B* **553** 229 (2003) [arXiv:hep-lat/0211043].
 73. For more conventional versions of “mixed” partial quenching, compare O. Bar, G. Rupak and N. Shoreh, *Phys. Rev. D* **67** 114505 (2003) [arXiv:hep-lat/0211050].
 74. S. Durr and C. Hoelbling, “Staggered versus overlap fermions: a study in the Schwinger model with $N_f = 0, 1, 2$,” arXiv:hep-lat/0311002.
 75. Weingarten and collaborators have discussed dynamical simulations with heavier fermions as corrections to the quenched approximation. See J. Sexton and D. Weingarten, *Phys. Rev. D* **55**, 4025 (1997) or W. J. Lee and D. Weingarten, *Phys. Rev. D* **59**, 094508 (1999) [arXiv:hep-lat/9811024].
 76. A. J. Buras, “Weak Hamiltonian, CP violation and rare decays,” arXiv:hep-ph/9806471.
 77. G. Martinelli and C. T. Sachrajda, *Nucl. Phys. B* **559**, 429 (1999) [arXiv:hep-lat/9812001]; For a review of modern “automated” technology, see H. D. Trotter, “Higher-order perturbation theory for highly-improved actions,” arXiv:hep-lat/0310044.
 78. S. J. Brodsky, G. P. Lepage and P. B. Mackenzie, *Phys. Rev. D* **28** 228 (1983).
 79. G. P. Lepage and P. B. Mackenzie, *Phys. Rev. D* **48** 2250 (1993) [arXiv:hep-lat/9209022]. See also G. Parisi, in *High Energy Physics—1980, XX Int. Conf., Madison (1980)*, ed. L. Durand and L. G. Pondrom (AIP, New York, 1981)
 80. See T. DeGrand, *Phys. Rev. D* **67** 014507 (2003) [arXiv:hep-lat/0210028]; W. j. Lee and S. R. Sharpe, *Phys. Rev. D* **66** 114501 (2002) [arXiv:hep-lat/0208018]; *Phys. Rev. D* **68** 054510 (2003) [arXiv:hep-lat/0306016].
 81. L. Maiani and G. Martinelli, *Phys. Lett. B* **178** 265 (1986).
 82. G. Martinelli, C. Pittori, C. T. Sachrajda, M. Testa and A. Vladikas, *Nucl. Phys. B* **445** 81 (1995) [arXiv:hep-lat/9411010].
 83. R. Sommer, *Nucl. Phys. Proc. Suppl.* **119**, 185 (2003) [arXiv:hep-lat/0209162].
 84. However, see G. M. de Divitiis, M. Guagnelli, R. Petronzio, N. Tantalo and F. Palombi, arXiv:hep-lat/0305018, G. M. de Divitiis, M. Guagnelli, F. Palombi,

- R. Petronzio and N. Tantalo, *Nucl. Phys.* **B 672** 372 (2003) [arXiv:hep-lat/0307005], for a renormalization-group-like analysis which connects quantities measured on a fine lattice with small volume, to large volume coarser lattices.
85. A. X. El-Khadra, A. S. Kronfeld and P. B. Mackenzie, *Phys. Rev.* **D 55** 3933 (1997) [arXiv:hep-lat/9604004];
A. S. Kronfeld, *Phys. Rev.* **D 62** 014505 (2000) [arXiv:hep-lat/0002008].
 86. C. T. H. Davies, K. Hornbostel, G. P. Lepage, A. J. Lidsey, J. Shigemitsu and J. H. Sloan, *Phys. Rev.* **D 52**, 6519 (1995) [arXiv:hep-lat/9506026]; *Phys. Lett.* **B 345** 42 (1995) [arXiv:hep-ph/9408328]. C. T. H. Davies, K. Hornbostel, A. Langnau, G. P. Lepage, A. Lidsey, J. Shigemitsu and J. H. Sloan, *Phys. Rev.* **D 50** 6963 (1994) [arXiv:hep-lat/9406017]; C. T. H. Davies *et al.*, *Phys. Rev. Lett.* **73** 2654 (1994) [arXiv:hep-lat/9404012]; and G. P. Lepage, L. Magnea, C. Nakhleh, U. Magnea and K. Hornbostel, *Phys. Rev.* **D 46** 4052 (1992) [arXiv:hep-lat/9205007].
 87. M. Wingate, J. Shigemitsu, C. T. Davies, G. P. Lepage and H. D. Trottier, *Phys. Rev.* **D 67** 054505 (2003) [arXiv:hep-lat/0211014]; J. Shigemitsu, C. T. Davies, A. Gray, E. Gulez, G. P. Lepage and M. Wingate, “Heavy-light meson semileptonic decays with staggered light quarks,” arXiv:hep-lat/0309039; M. Wingate, C. Davies, A. Gray, E. Gulez, G. P. Lepage and J. Shigemitsu, “Progress calculating decay constants with NRQCD and AsqTad actions,” arXiv:hep-lat/0309092.
 88. D. Becirevic and J. Reyes, “HQET with chiral symmetry on the lattice,” arXiv:hep-lat/0309131.
 89. C. W. Bernard, *Nucl. Phys. Proc. Suppl.* **94** 159 (2001) [arXiv:hep-lat/0011064].
 90. C. Bernard *et al.*, *Phys. Rev.* **D 65** 014510 (2002) [arXiv:hep-lat/0109015].
 91. M. Della Morte, S. Durr, J. Heitger, H. Molke, J. Rolf, A. Shindler and R. Sommer [ALPHA Collaboration], “Static quarks with improved statistical precision,” arXiv:hep-lat/0309080.
 92. A. S. Kronfeld and S. M. Ryan, *Phys. Lett.* **B 543** 59 (2002) [arXiv:hep-ph/0206058].
 93. C. Bernard *et al.*, *Nucl. Phys. Proc. Suppl.* **119** 170 (2003) [arXiv:hep-lat/0209086].
 94. D. Becirevic, S. Fajfer, S. Prelovsek and J. Zupan, *Phys. Lett.* **B 563** 150 (2003) [arXiv:hep-ph/0211271].
 95. A. Anastassov *et al.* [CLEO Collaboration], *Phys. Rev.* **D 65** 032003 (2002) [arXiv:hep-ex/0108043].
 96. S. M. Ryan, *Nucl. Phys. Proc. Suppl.* **106**, 86 (2002) [arXiv:hep-lat/0111010].
 97. H. Wittig, “Status of lattice calculations of B-meson decays and mixing,” arXiv:hep-ph/0310329.
 98. D. Becirevic, “Status of the computation of $f(B/s,d)$, ξ and g ,” arXiv:hep-ph/0310072.
 99. A. S. Kronfeld, “Heavy quarks and lattice QCD,” arXiv:hep-lat/0310063.
 100. C. Bernard *et al.* [MILC Collaboration], *Nucl. Phys. Proc. Suppl.* **119** 613 (2003) [arXiv:hep-lat/0209163].
 101. S. Hashimoto, A. X. El-Khadra, A. S. Kronfeld, P. B. Mackenzie, S. M. Ryan and J. N. Simone, *Phys. Rev.* **D 61** 014502 (2000) [arXiv:hep-ph/9906376]; S. Hashimoto, A. S. Kronfeld, P. B. Mackenzie, S. M. Ryan and J. N. Simone, *Phys. Rev.* **D 66** 014503 (2002) [arXiv:hep-ph/0110253].
 102. N. Isgur and M. B. Wise, *Phys. Lett.* **B 232** 113 (1989); *Phys. Lett.* **B 237** 527 (1990).
 103. A. F. Falk and M. Neubert, *Phys. Rev.* **D 47** 2965 (1993) [arXiv:hep-ph/9209268]; T. Mannel, *Phys. Rev.* **D 50** 428 (1994) [arXiv:hep-ph/9403249].
 104. S. Aoki *et al.* [JLQCD Collaboration], “B0 anti-B0 mixing in unquenched lattice QCD,” arXiv:hep-ph/0307039.

105. M. Wingate, C. Davies, A. Gray, E. Gulez, G. P. Lepage and J. Shigemitsu, “Progress calculating decay constants with NRQCD and AsqTad actions,” arXiv:hep-lat/0309092; “The B_s and D_s decay constants in 3 flavor lattice QCD,” arXiv:hep-lat/0311130.
106. For examples of global fits to the CKM matrix, see A. Hocker, H. Lacker, S. Laplace and F. Le Diberder, *Eur. Phys. J. C* **21** 225 (2001) [arXiv:hep-ph/0104062].
107. R. Gupta, T. Bhattacharya and S. R. Sharpe, *iPhys. Rev. D* **55** 4036 (1997) [arXiv:hep-lat/9611023].
108. S. Aoki *et al.* [JLQCD Collaboration], *iPhys. Rev. Lett.* **81** 1778 (1998) [arXiv:hep-lat/9705035].
109. L. Conti, A. Donini, V. Gimenez, G. Martinelli, M. Talevi and A. Vladikas, *iPhys. Lett. B* **421** 273 (1998) [arXiv:hep-lat/9711053].
110. S. Aoki *et al.* [JLQCD Collaboration], *Phys. Rev. D* **60** 034511 (1999) [arXiv:hep-lat/9901018].
111. G. Kilcup, R. Gupta and S. R. Sharpe, *Phys. Rev. D* **57** 1654 (1998) [arXiv:hep-lat/9707006].
112. S. Aoki *et al.* [JLQCD Collaboration], *Phys. Rev. Lett.* **80** 5271 (1998) [arXiv:hep-lat/9710073].
113. T. Bhattacharya, G. T. Fleming, G. Kilcup, R. Gupta, W. Lee and S. Sharpe, “Calculating weak matrix elements using HYP staggered fermions,” arXiv:hep-lat/0309105.
114. A. Ali Khan *et al.* [CP-PACS Collaboration], *Phys. Rev. D* **64** 114506 (2001) [arXiv:hep-lat/0105020].
115. T. Blum *et al.* [RBC Collaboration], “Kaon matrix elements and CP-violation from quenched lattice QCD. I: The 3-flavor case,” arXiv:hep-lat/0110075.
116. S. Capitani and L. Giusti, *Phys. Rev. D* **62** 114506 (2000) [arXiv:hep-lat/0007011].
117. N. Garron, L. Giusti, C. Hoelbling, L. Lellouch and C. Rebbi, “B(K) from quenched QCD with exact chiral symmetry,” arXiv:hep-ph/0306295.
118. T. DeGrand [MILC collaboration], “Kaon B-parameter using overlap fermions,” arXiv:hep-lat/0208054.
119. T. Izubuchi [the RBC Collaboration], “B(K) from two-flavor dynamical domain wall fermions,” arXiv:hep-lat/0310058.
120. M. Golterman and E. Pallante, *JHEP* **0008**, 023 (2000) [arXiv:hep-lat/0006029]; *JHEP* **0110** 037 (2001) [arXiv:hep-lat/0108010].
121. A. J. Buras, “CP violation in B and K decays: 2003,” arXiv:hep-ph/0307203.
122. A. Lai *et al.* [NA48 Collaboration], *Eur. Phys. J. C* **22** 231 (2001) [arXiv:hep-ex/0110019]; J. R. Batley *et al.* [NA48 Collaboration], *Phys. Lett. B* **544** 97 (2002) [arXiv:hep-ex/0208009].
123. A. Alavi-Harati *et al.* [KTeV Collaboration], *Phys. Rev. Lett.* **83** 22 (1999) [arXiv:hep-ex/9905060]; *Phys. Rev. D* **67** 012005 (2003) [arXiv:hep-ex/0208007].
124. H. Burkhardt *et al.* [NA31 Collaboration], *Phys. Lett. B* **206** 169 (1988); G. D. Barr *et al.* [NA31 Collaboration], *Phys. Lett. B* **317** 233 (1993).
125. L. K. Gibbons *et al.*, *Phys. Rev. Lett.* **70** 1203 (1993).
126. J. I. Noaki *et al.* [CP-PACS Collaboration], *Phys. Rev. D* **68** 014501 (2003) [arXiv:hep-lat/0108013].
127. This can’t be done directly: L. Maiani and M. Testa, *Phys. Lett. B* **245** 585 (1990). However, by studying systems in finite volumes near avoided level crossings, final state interactions can be determined. See L. Lellouch and M. Luscher, *Commun. Math. Phys.* **219** 31 (2001) [arXiv:hep-lat/0003023].
128. Y. Kuramashi, *Nucl. Phys. Proc. Suppl.* **83** 24 (2000) [arXiv:hep-lat/9910032].
129. C. W. Bernard, T. Draper, A. Soni, H. D. Politzer and M. B. Wise, *Phys. Rev. D*

- 32** 2342 (1985).
130. C. Bernard, in the *Proceedings of the 1989 TASI Summer School*, eds. T. DeGrand and D. Toussaint, (World Scientific, Singapore, 1989).
131. S. Aoki *et al.* [JLQCD Collaboration], *Phys. Rev. D* **58**, 054503 (1998) [arXiv:hep-lat/9711046].